Light Propagation in Generalized Lens-Like Media

By S. E. MILLER

(Manuscript received July 23, 1965)

This paper provides a preliminary assessment of electromagnetic wave propagation in focusing media which departs from those previously studied, ideal lenses and continuous media with square-law index variation. New approximate methods are described for obtaining the transverse beam width, phase constant, and ray trajectory in continuous lens-like media, and for determining stability conditions in lens waveguides, where the lenses contain spherical aberration and the continuous media contain fourth-order or higher-order terms of variation in index of refraction.

It is proven that only in aberrationless-tens waveguides or in a continuous medium with square-law index variation will the shape of a beam injected off axis or with an angle to the medium's axis remain constant about a beam axis which oscillates about the axis of the medium. In non-square law media the beam will spread, but knowledge of the coefficients describing the medium and the position and angle of the injected beam enables one to specify the maximum radius within which all of the energy will be confined.

The following is an example of the type of solution obtained for non-square law media: for a medium characterized by the transverse index variation

$$n = n_a\ (1 - \tfrac{1}{2}a_4x^4)$$

and assuming no index variation exists in the direction of propagation, the radius to the $1/e$ *point in field is approximately*

$$w_e = 0.666\,\frac{\lambda^{1/3}}{a_4^{1/6}}$$

and the phase constant is

$$\beta = \frac{2\pi}{\lambda} - \frac{0.256\ (a_4\lambda)^{1/3}(m+1)^2}{\left(\dfrac{m+2.5}{2.5}\right)^{2/3}}$$

where the free-space wavelength $\lambda_0 = n_a\lambda$ *and* m *is the order of the mode,* $m = 0, 1, 2 \cdots$ *. Quite generally, non-square law media show dispersion, and unlike the square-law media the various modes travel with different group velocities. Expressions are given to allow these effects to be evaluated for small perturbations on a square-law medium as well as for higher-order index variations.*

The transverse beam shape associated with any law of index variation is shown to be as well approximated (in the region of significant power density) by a cosine function or Gaussian function as is the field for an ideal lens-waveguide approximated by a Gaussian function in the presence of typical diffraction losses.

Normal mode shapes are obtained for resonators with fourth-order and eighth-order mirrors by the method of Fox and Li; diffraction losses for a few Fresnel numbers are also given. In a certain range of Fresnel numbers, fourth- and eighth-order mirrors give lower diffraction losses than spherical mirrors.

An approximate method for solving the paraxial ray equation for rather general (non-square-law) media is outlined. Requiring only reciprocity and symmetry about the medium's axis, it is shown that the radial position of the ray (x) *is related to distance* (z) *along the axis of the medium by*

$$x = \Sigma b_m \cos m\beta z$$

where $m = 1, 3, 5, 7 \cdots$ *. Moreover, it is shown that this series converges very rapidly, making it possible to get a good approximate representation with only a few terms. For example, for the fourth-order medium described above, an approximate solution is*

$$x = x_0 \{0.959 \cos \beta z + 0.041 \cos 3\beta z\}$$

where $\beta = x_0 \sqrt{1.44a_4}$ *. It is characteristic of all non-square law media to have a ray period* $2\pi/\beta$ *which is a function of the peak ray displacement,* x_0 *.*

Lens waveguides with fourth- or higher-order terms in the focusing or index function can of course exhibit increasingly strong focusing for energy departing farther from the medium's axis, and if the lenses are suitably spaced might be useful in reducing the magnitude of beam wander due to imperfections or guide-axis curvature. However, for a given beam spot size, non-square-law lenses must be placed closer together than square-law lenses.

Use of non-square law lenses or distributed media in transmission systems will most probably require repeater-system techniques which are operable with multi-mode signals at the receiver input.

I. INTRODUCTION

Although a great deal of work has been done to describe electromagnetic wave guidance using a sequence of ideal aberrationless lenses, little has been done with more general lens-like media. The objective of this paper is to provide a beginning understanding of what happens to the important descriptive parameters of a light waveguide—wave phase constant, wave spot size, ray trajectory, stability restrictions—for general lens-like media, either continuous or formed from a sequence of focusing elements. Exact solutions for these parameters are difficult or impossible, a possible reason for little having been done.* A second result presented herein is a series of analytical techniques for obtaining useful approximate solutions representing a broad class of lens-like media; some of these techniques are most clearly presented by giving examples, which unfortunately leads to a rather large number of equations. To aid the reader in finding the section dealing with a particular topic, an outline and brief resume is given below.

As pointed out by J. W. Tukey, there is no *a priori* reason why ideal aberrationless lenses are best for use as a communication medium. We would like to know what does happen to wave guidance as we depart from aberrationless lenses, which is the case studied extensively in earlier work. Gas lenses have nearly constant focal length but their "principal planes" are actually curved surfaces.[1] E. A. Marcatili and D. H. Ring have pointed out that these curved principal planes have effects similar to those expected in plane lenses with spherical aberration. Thus the present work relates to existing gas lenses as well as to the question of whether or not to attempt to create a different form of inhomogeneous medium for light-wave guidance.

Some of the present work dates back more than a year; impetus to putting it on paper was given by recent calculations planned by E. A. Marcatili and D. Marcuse.[2] These calculations showed that ray optics can accurately predict the loss even when half of the beam falls off the edge of the lens. Many of the conclusions drawn here are based on ray optics but since the controlling transverse variations take place over distances that are large compared to the wavelength, ray optics should give a correct conclusion.

The subject is developed in this paper in the following manner. Section II covers ray optics for aberrationless lenses of any thickness, in-

* As this paper goes into print, S. J. Buchsbaum points out the existence of an exact solution for a particular non-square-law $f(x)$ originally derived with reference to a quantum-mechanical problem. J. P. Gordon will report on this in a later publication.

cluding the case of a continuous medium. A ray-optic method for determining stability conditions applicable (using results of later sections) with generalized focusing elements is also covered here. Proof that the transverse field distribution of a normal mode beam injected off the medium's axis (or which goes there due to curvature, or displacement of the medium) is preserved only when the index of refraction decreases as the square of the distance off axis is presented in Section III. Section IV develops the proof that in a wide class of continuous focusing media, the ray paths are representable by a series of odd-harmonic cosine or sine terms. A definition of the focal length of a segment of an arbitrary medium is covered in Section V. Section VI discusses a new technique for obtaining approximately the wave phase constant and spot size for generalized lens-like media, stated generally and illustrated for fourth-order and eighth-order media. A characteristic ray angle and a characteristic ray period is defined for the generalized medium. Calculations for field distribution and diffraction losses in resonators and lens waveguides using non-square-law elements are derived in Section VII. These calculations are the only ones available on fields and losses in non-square-law resonators. Section VIII discusses a solution for ray paths in pure fourth-order, or a mixture of second- and fourth-order, media; the approach for extension to other media is indicated. Some further discussion and acknowledgements are presented in Section IX.

II. TRANSMISSION IN AN IDEAL LENS-LIKE MEDIUM

The medium referred to as ideal is one in which the index of refraction has the form[3] (see Fig. 1a)

$$n = n_a\,(1 - \tfrac{1}{2}a_2x^2) \tag{1}$$

where

n_a = index of refraction on axis, $x = 0$
x = transverse dimension
a_2 = a constant.

The index is independent of z,

$$\partial n/\partial z = 0. \tag{2}$$

We can obtain a solution for the path of a light ray in such a medium using the well known paraxial ray equation

$$\frac{\partial^2 x}{\partial z^2} = \frac{1}{n}\frac{\partial n}{\partial x}. \tag{3}$$

Here, x is the position of the ray at some value of z. Equation (3) is

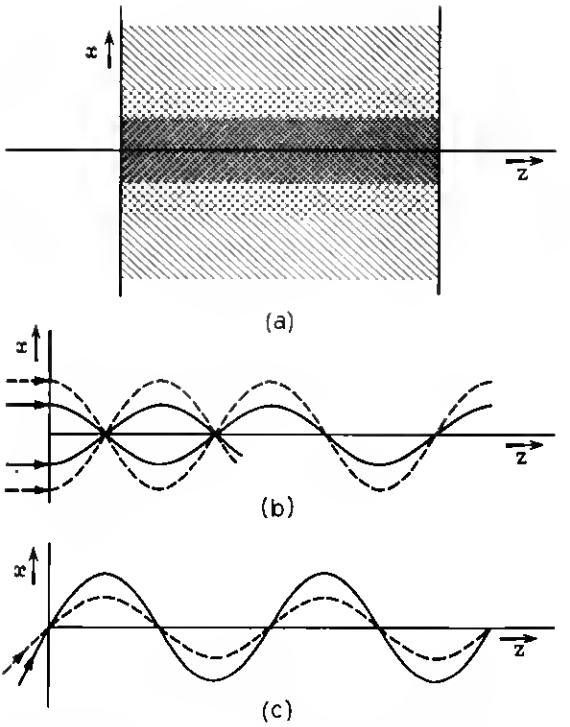

Fig. 1 — Ideal lens-like medium, (a)—two-dimensional continuous medium with index of refraction independent of z and varying with x according to (1), (b)—light ray paths in medium a for parallel input rays, (c)—light ray paths in medium a with non-parallel input rays.

valid over a broad range of conditions provided only that the ray path makes a small angle to the z-axis. For a medium of the form of (1)

$$\frac{\partial n}{\partial x} = -n_a a_2 x \tag{4}$$

and with the restriction

$$|\tfrac{1}{2} a_2 x^2| \ll 1 \tag{5}$$

we can write

$$\frac{\partial^2 x}{\partial z^2} = \frac{1}{n}\frac{\partial n}{\partial x} = -a_2 x. \tag{6}$$

The general form of (6) indicates an exponential solution for x as a function of z, and it can be verified that

$$x = A \cos \sqrt{a_2}\, z + B \sin \sqrt{a_2}\, z \tag{7}$$

is a solution, A and B being constants to be determined.

Using the boundary conditions at $z = 0$,

$$x = r_i = \text{input ray position} \tag{8}$$

$$\frac{\partial x}{\partial z} = r_i' = \text{input ray slope.} \tag{9}$$

We have

$$x = r_i \cos \sqrt{a_2}\, z + r_i' \sqrt{1/a_2} \sin \sqrt{a_2}\, z. \tag{10}$$

This is very interesting in that it corresponds exactly to the ray behavior in a sequence of equally spaced aberrationless lenses.[4,5] It is important that all rays have the same oscillatory period regardless of input displacement or input slope, as sketched in Figs. 1(b) and 1(c). It is likewise significant that the effects of input ray slope and position are separable with respect to x, subsequent ray position.

If a_2 is negative, the cosine and sine of (10) become cosh and sinh and a divergent medium results.

A short segment of the distributed medium characterized by (1) may be assigned an equivalent focal length, even when it is not a "thin" or "weak" lens. With reference to Fig. 2, the most general case is one in which the index on axis, n_a, is different from that of the surrounding

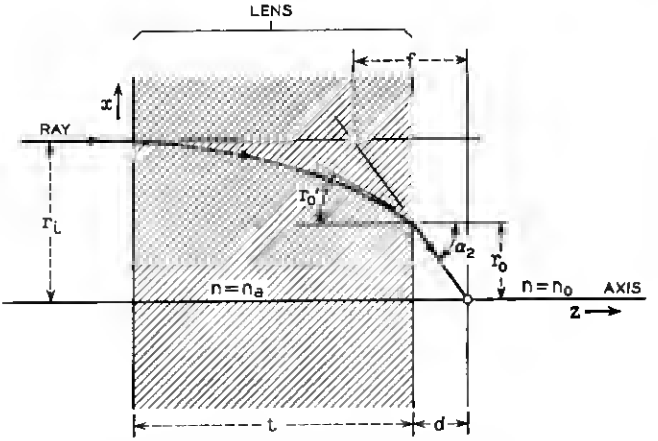

Fig. 2 — Diagram defining focal length and principal plane for an ideal distributed lens.

medium n_0. The path of input ray with zero slope and displacement r_i can be obtained from (10).

The general equation for the ray slope, derived from (10), is

$$\frac{dx}{dz} = -r_i \sqrt{a_2} \sin \sqrt{a_2}\, z + r_i' \cos \sqrt{a_2}\, z. \tag{11}$$

At the lens output the displacement is

$$r_0 = r_i \cos \sqrt{a_2}\, t \tag{12}$$

and the ray slope is, from (11),

$$r_0' = -r_i \sqrt{a_2} \sin \sqrt{a_2}\, t. \tag{13}$$

Because (5) holds, the refraction at the lens output surface is (see Fig. 2)

$$\frac{r_0'}{\alpha_2} = \frac{n_0}{n_a}. \tag{14}$$

Hence,

$$d = \left| \frac{r_0}{\alpha_2} \right| = \left| \frac{n_0 \cot \sqrt{a_2}\, t}{n_a \sqrt{a_2}} \right|. \tag{15}$$

The distance from the focal point to the principal plane where an equivalent thin lens may be placed (Fig. 2) is

$$f = \frac{r_i}{\alpha_2} = \frac{n_0}{n_a \sqrt{a_2} \sin \sqrt{a_2}\, t}. \tag{16}$$

This result was excerpted from the present work and given previously[6] with the approximation appropriate to gas lenses $n_0 \cong n_a$.

With the continuous focusing medium according to (1), there is no limit to the strength of the focusing effect; a stronger index gradient merely confines the normal mode energy more closely to the axis. However, when a series of segments of the distributed medium are used as a waveguide, with gaps of a homogeneous medium in-between, there is a cut-off effect which occurs if the lenses are too strong in relation to the lens spacing. This is a well-known effect with thin lenses,[4] and the limiting conditions were derived from wave optics for the medium according to (1) by J. R. Pierce[3] and E. A. Marcatili.[7] A ray-optic derivation is given here for the medium (1) to show the method which can be extended to arbitrary focusing media, including fourth-order or higher-order terms in x, which has not yet been handled by wave optics.

With reference to Fig. 3(a), we assume an input ray of zero slope and a displacement r_i at the center of the first lens, where the longitudinal axis $z_1 = 0$. At $z_1 = t/2$ and restricting our attention momentarily to the regiou $0 < \sqrt{a_2}\, t < \pi/2$, the output of lens # 1 is

$$r_{01} = r_i \cos(\sqrt{a_2}\, t/2) \tag{17}$$

$$r_{01}' = -r_i \sqrt{a_2} \sin(\sqrt{a_2}\, t/2). \tag{18}$$

Taking the approximation appropriate to gas lenses, $n_0 \cong n_a$, the ray output of lens 1 intersects the axis at a distance $b/2$ from the end of lens # 1 (Fig. 3a).

$$b/2 = |\, r_{01}/r_{01}' \,|. \tag{19}$$

Using our knowledge that (1) is symmetrical about $x = 0$ and reciprocity holds, we can construct the remainder of Fig. 3(a) with a ray maximum r_i at the center of the second lens. The value of b corresponding to this condition is

$$b = \frac{2}{\sqrt{a_2}} \cot(\sqrt{a_2}\, t/2). \tag{20}$$

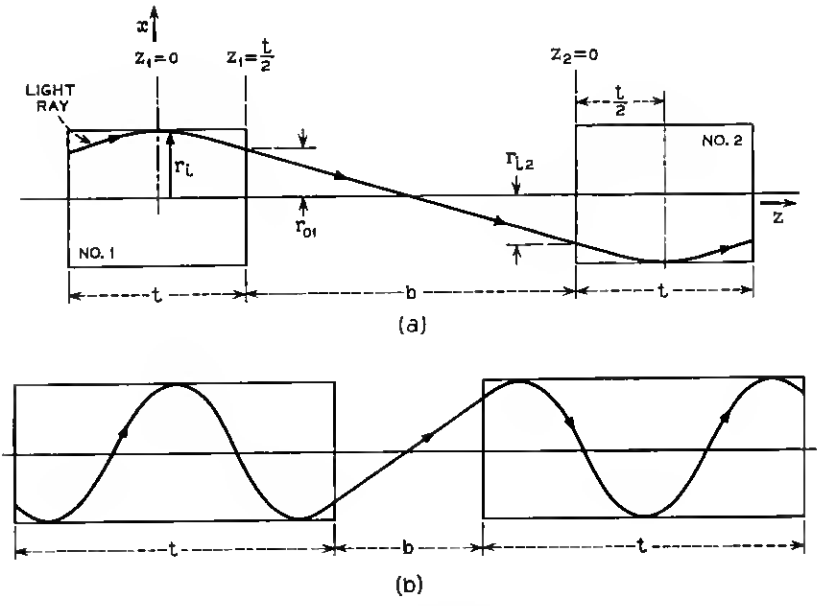

Fig. 3 — Ray path at one maximum lens spacing, (a)—weakest lens case, (b)—second stability band (stronger lenses than 3a).

It is clear that this is the largest permissible ray displacement at the center of lens #2, since a larger value there would represent displacement growth without limit as $z \to \infty$. We can show that larger values of b violate this stability condition by writing the expression for the displacement at the center of the second lens. The input to the second lens is

$$\text{slope} \qquad r_{i2}' = r_{01}' \tag{21}$$

$$\text{displacement} \quad r_{i2} = r_{01} + br_{01}'. \tag{22}$$

Then, from (10) and using a new origin of the longitudinal axis $z_2 = 0$ at the input to the second lens,

$$x_2 = r_{i2} (\cos \sqrt{a_2}\, z_2) + \frac{r_{i2}'}{\sqrt{a_2}} \sin \sqrt{a_2}\, z_2. \tag{23}$$

Using (21) and (22)

$$\frac{x_2}{r_i} = \cos (\sqrt{a_2}\, z) \{\cos (\sqrt{a_2}\, t/2) - b \sqrt{a_2} \sin (\sqrt{a_2}\, t/2)\} - \sin (\sqrt{a_2}\, z_2) \sin (\sqrt{a_2}\, t/2). \tag{24}$$

Making the substitution

$$b = \frac{2}{\sqrt{a_2}} \cot (\sqrt{a_2}\, t/2) + \delta \tag{25}$$

and evaluating (24) at $z_2 = t/2$ we find

$$\left.\frac{x_2}{r_i}\right|_{z_{i2}=t/2} = -[1 + \delta \sin (\sqrt{a_2}\, t/2) \cos (\sqrt{a_2}\, t/2)]. \tag{26}$$

In the region $0 < \sqrt{a_2}\, t/2 < \pi/2$ both $\sin (\sqrt{a_2}\, t/2)$ and $\cos (\sqrt{a_2}\, t/2$ are positive; hence for δ positive, the ray at the center of the second lens is displaced more than the input ray and a divergent path is followed in such a sequence of lenses. For δ negative the propagation is stable. For $\pi < \sqrt{a_2}\, t/2 < 3\pi/2$ another passband occurs with the limiting value of b having a ray path as in Fig. 3(b). This leads to the stability conditions

$$b \leqq \frac{2}{\sqrt{a_2}} \cot (\sqrt{a_2}\, t/2) \tag{27}$$

applicable in the regions of lens length

$$n\pi < \sqrt{a_2}\, t/2 < n\pi + \frac{\pi}{2} \tag{28}$$

where $n = 0, 1, 2, 3$, etc.

For other permissible values of lens length we derive the stability condition with reference to Fig. 4. The input ray at $z_1 = 0$, center of lens #1, has zero displacement and a slope of r_i'. Fig. 4(*a*) shows the ray path for the limiting value of b when $\pi/2 < \sqrt{a_2}\, t/2 < \pi$, constructed using symmetry and reciprocity as before. This yields

$$b = -\frac{2}{\sqrt{a_2}} \tan\left(\sqrt{a_2}\, t/2\right). \tag{29}$$

This gives a positive value for b because the tangent is negative. Following the lines indicated above we can derive an expression for the ray path in lens #2

$$x_2 = \cos\left(\sqrt{a_2}\, z_2\right)\left\{\frac{r_i'}{\sqrt{a_2}} \sin\left(\sqrt{a_2}\, t/2\right) + b r_i' \cos\left(\sqrt{a_2}\, t/2\right)\right\} + \frac{r_i'}{\sqrt{a_2}} \cos\left(\sqrt{a_2}\, t/2\right) \sin\left(\sqrt{a_2}\, z\right). \tag{30}$$

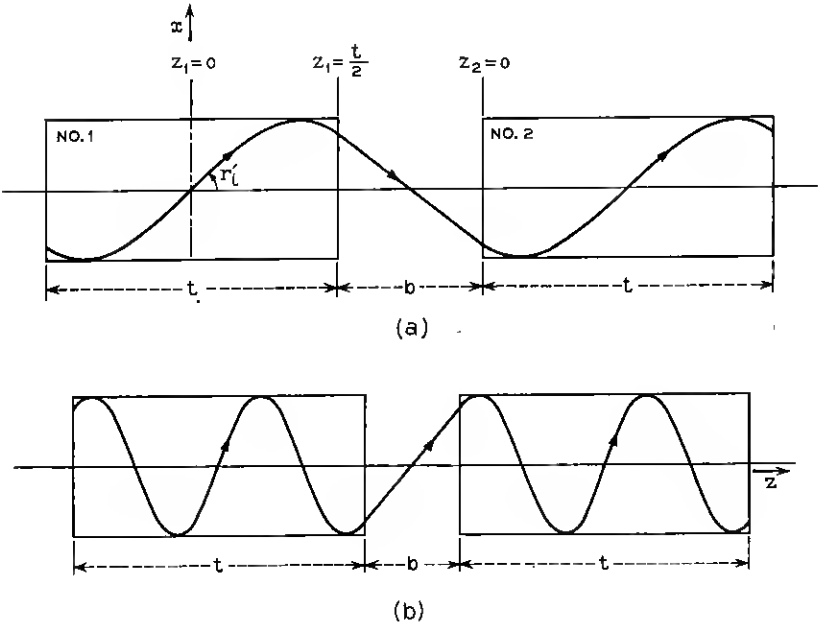

Fig. 4 — Ray path at another maximum lens spacing, (a)—weak lens case (b)—second stability band (stronger lenses than 4a).

We want the slope at the middle of this lens, which is obtained by putting $z_2 = t/2$ in

$$\frac{dx_2}{dz_2} = -\sqrt{a_2}\sin(\sqrt{a_2}\,z)\left\{\frac{r_i'}{\sqrt{a_2}}\sin(\sqrt{a_2}\,t/2) + br_i'\cos(\sqrt{a_2}\,t/2)\right\} + r_i'\cos(\sqrt{a_2}\,t/2)\cos(\sqrt{a_2}\,z)\,. \tag{31}$$

Letting

$$b = -\frac{2}{\sqrt{a_2}}\tan(\sqrt{a_2}\,t/2) + \delta \tag{32}$$

we obtain

$$\left.\frac{1}{r_i'}\frac{dx_2}{dz_2}\right|_{z_2=t/2} = 1 - \delta\sqrt{a_2}\sin(\sqrt{a_2}\,t/2)\cos(\sqrt{a_2}\,t/2). \tag{33}$$

In the region $\pi/2 < (\sqrt{a_2}\,t/2) < \pi$, the sine term is positive and the cosine term is negative; hence a positive δ indicates instability, a slope at the center of the second lens greater than the slope at the center of the first lens and (as may be verified in (30)) a displacement at $z_2 = t/2$ adding to the subsequent ray divergence.

Higher order passbands occur, one sketched in Fig. 4(b). Thus, in the region

$$(n\pi + \pi/2) < (\sqrt{a_2}\,t/2) < (n+1)\pi$$

$n = 0, 1, 2, 3, 4$, etc., the permitted range of lens spacing b is

$$b \leqq -\frac{2}{\sqrt{a_2}}\tan(\sqrt{a_2}\,t/2). \tag{34}$$

Equations (27) and (34) are identical to the relations obtained from wave theory.[7]

The above method for determining stability of lens waveguides can be applied for arbitrarily shaped lenses, as long as symmetry about the z axis and reciprocity exist. Numerical integration can be employed where the lens cannot easily be represented by functions in closed form.[1]

III. WAVE BEHAVIOR IN INHOMOGENEOUS MEDIA

We will now consider media which are of the form

$$n = n_a[1 + f(x)] \tag{35}$$

where

$$f(x) = -\tfrac{1}{2}a_2x^2 - \tfrac{1}{2}a_4x^4 - \tfrac{1}{2}a_6x^6 \cdots \tag{36}$$

in which a_2, a_4, $a_6 \cdots$ are constants which may be positive or negative. Positive values represent convergent focusing and negative values represent divergent focusing. This represents a general medium restricted only to symmetry about the axis $x = 0$ and uniform with respect to the direction of propagation.

The normal mode for such a medium is characterized by the index variation. We will presently discuss the field shapes and losses for several special cases of (35); for now it is sufficient to note that a *different* equation for the index n means a different normal mode.

An interesting general conclusion can be drawn by expanding the index n of (35) about some off-axis radius r_1 as in Fig. 5:

$$\begin{aligned}\frac{n(x - r_1)}{n_a} = \frac{n(x')}{n_a} = \frac{n(x = r_1)}{n_a}\\ + x'\{-a_2r_1 - 2a_4{r_1}^3 - 3a_6{r_1}^5 \cdots\}\\ + \frac{(x')^2}{2}\{-a_2 - 6a_4{r_1}^2 - 15a_6{r_1}^4 \cdots\}\\ + \frac{(x')^3}{6}\{-12a_4r_1 - 60a_6{r_1}^3 \cdots\}\\ + \frac{(x')^4}{24}\{-12a_4 - 180a_6{r_1}^2 \cdots\}\end{aligned} \tag{37}$$

in which

$$x' = (x - r_1).$$

With the approximation

$$f(x) \ll 1 \tag{38}$$

the first term of (37) is unity. Then for a_4, a_6, and all higher order coefficients equal to zero, (37) becomes

$$n(x') = n_a\{1 - a_2r_1x' - \tfrac{1}{2}a_2(x')^2\}. \tag{39}$$

This is sketched in Fig. 5. Thus, for the medium according to (1), the effect of entering off axis at $x = r_1$ instead of at $x = 0$ is to introduce a term in the index which is linear in x. This term has the effect of delaying or advancing every region of the transverse cross section an amount proportional to the displacement from the axis; this term

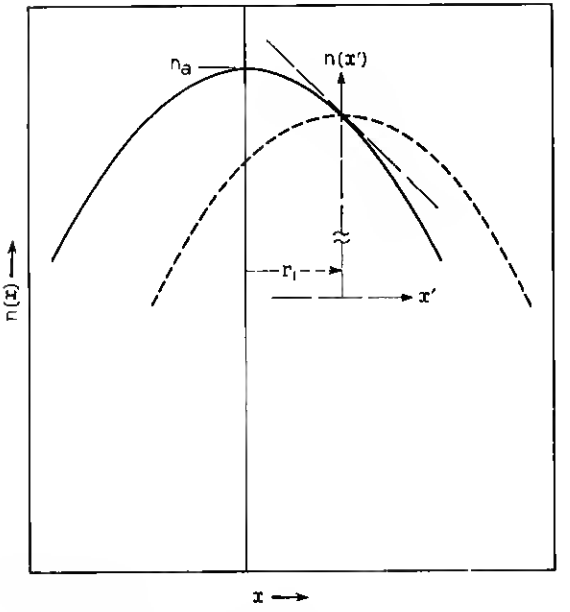

Fig. 5 — Expansion of $n(x)$ about point $x = r_1$.

acts the same as a dielectric wedge and tilts the wave front. The path of any ray is described by ray optics in the continuous medium according to (10). The remaining term of (39) is identical to the original equation at $r_1 = 0$; hence the normal mode for a wave entering at $x = r_1$ is the same as at $x = 0$, with a direction change superimposed.* Thus, the beam follows a path sketched as in Fig. 6(a); a pure mode introduced into the square-law medium travels without change of shape if the change in position and direction of the beam axis is taken into account. If a plane wave is introduced, Fig. 6(b), the field is concentrated periodically at the points where the beam axis crosses the axis of the medium.

We can also see immediately that these properties are *not* characteristic of any medium in which a_4 or higher order terms are present. In the expansion (37) there are, in addition to the term linear in x', additional terms in $(x')^2$ and $(x')^3$ brought in by a_4, a_6, etc., which change the normal modes in a manner dependent on the particular value of r_1. When any one or more of a_4, a_6, etc., are non-zero, the

* This was previously proven for a sequence of ideal lenses independently by H. E. Rowe and J. P. Gordon.

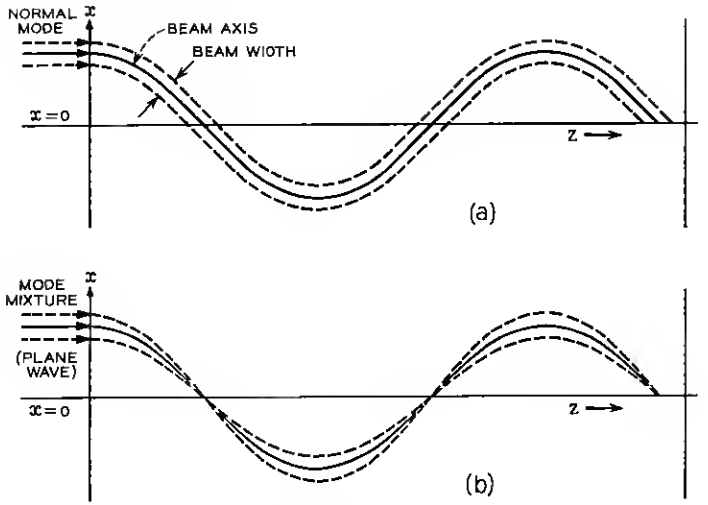

Fig. 6 — Ray path representation of beam flow in the ideal square law-medium, (a)—normal mode off-axis input, (b)—mode mixture off-axis input.

modes for a region off the axis of the medium are different from tbose on axis and the rather simple and attractive situation sketched in Fig. 6 no longer exists. It also follows that ray paths also differ importantly from those sketched in Figs. 1 (b) and 1 (c).

IV. RAY PATHS IN NON-SQUARE-LAW MEDIA

When $f(x)$ of (35) and (36) contain non-zero a_4 or higber order terms, the general shape of $f(x)$ can be something like that of Fig. 5, even thougb a_4 or some other terms are negative yielding a defocusing tendency. We shall be concerned now with arbitrary values of a_2, a_4, a_6, etc., within the limits on x such that

$$\begin{aligned} \frac{df(x)}{dx} \quad &< 0 \quad \text{for } x > 0 \\ &> 0 \quad \text{for } x < 0 \end{aligned} \tag{40}$$

Tbis assures that all rays will be bent toward the axis at any x, per (3).

We can observe several additional features of the general case:

(1.) As a consequence of (40), any ray will monotonically go through a maximum and return to the axis, as sketched in Fig. 7. Due to symmetry about the z axis and reciprocity, the curve $x = g(z)$ will have even symmetry about z_2, z_4, etc. and odd symmetry about z_3, z_5, etc. The period of g(z), $(z_5 - z_1)$, will depend on the coefficients a_2, a_4, $\cdots$ in (36).

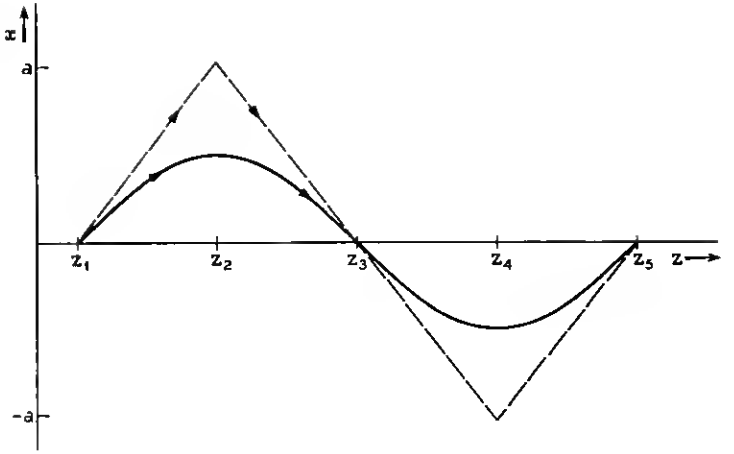

Fig. 7 — Ray paths in a generalized lens-like medium.

(2.) It will be instructive to note that

$$f(x) = -\left|\frac{x}{a}\right|^m \tag{41}$$

with $m \to \infty$ is the special case of (36) which corresponds to a step change in index at $|x| = a$:*

$$\begin{aligned} f(x) &\to 0 \quad \text{and} \quad n = n_a \quad \text{for } |x| < |a| \\ -f(x) &\gg 0 \quad \text{and} \quad (n-1) \ll (n_a - 1) \quad \text{for } |x| \to |a|. \end{aligned} \tag{42}$$

We will see that this is a convenient bounding condition on non-ideal focusing media. In Fig. 7, the dotted line represents the ray path for such a medium.

(3.) As already noted, the paraxial ray equation (3) is valid. Since $f(x)$ in (36) is to be kept very small compared to unity, the solution for the position of the ray as a function of z, $x = g(z)$, is related

$$\frac{d^2}{dz^2}[g(z)] = \frac{1}{n}\frac{\partial n}{\partial x} = \frac{d}{dx}[f(x)] \tag{43}$$

or

$$f(x) = \int \frac{d^2}{dz^2}[g(z)]\, dx. \tag{44}$$

* We will want to continue to use the paraxial ray equation and the associated condition, $f(x) \ll 1$. We shall use the region $0 < |x| < a$ but allow $|x|$ to approach a so closely that $f(x) \gg 0$.

(4.) Due to symmetry about the z axis,

$$\frac{d^2}{dz^2}[g(z)] = 0 \text{ at values of } z \text{ where } x = g(z) = 0. \tag{45}$$

Obviously,

$$\frac{d}{dz}[g(z)] = 0 \tag{46}$$

periodically at maxima for $g(z)$, which will occur at values of z midway between the places where $g(z) = 0$, Fig. 7.

(5.) It follows from the preceding notes that the function $g(z)$ must have even symmetry about the values of z for which (46) holds, and odd symmetry about the values of z for which $g(z) = 0$, a consequence of reciprocity and the known symmetry about $x = 0$ for $f(x)$. Hence, the most general ray trajectory will be of the form

$$x = \sum_{1}^{\infty} b_m \cos m\beta z \tag{47}$$

where $m = 1, 3, 5, 7, \cdots$ etc. We will proceed presently to find a particular solution of the form (47).

In all functions (35) where a_4 or some higher a_n is present, the period of the ray trajectory depends on the peak amplitude. That is, if the medium characterized by (35) starts at $z = 0$ (as in Fig. 8) and if a series of rays enter parallel to the z axis but at different values of x, the ray trajectories will have different periods. If a_2, a_4, etc. are all positive, the rays farther from the z axis will be bent more sharply and the picture qualitatively will be as sketched in Fig. 8. However, if a_2

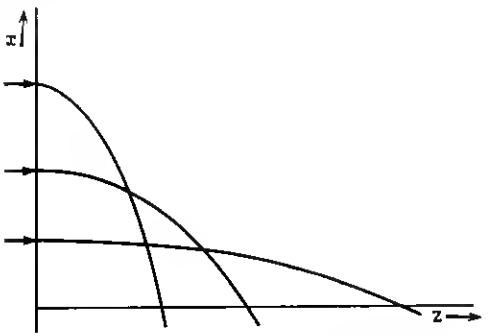

Fig. 8 — Ray paths in a generalized focusing medium for various parallel input rays.

is positive and a_4 negative (other $a_n = 0$) the rays entering farther from the z axis will have a period *longer* than those entering near the z axis. As previously noted, all rays have the same period (Fig. 1) only when all a_n except a_2 are zero.

V. FOCAL LENGTH OF A SEGMENT OF AN ARBITRARY MEDIUM

Suppose a ray at radius x passes through a section of arbitrary medium (Fig. 1a) of length t. We can ascribe a focal length to each x position as follows: the phase difference $\Delta\varphi$ between a ray *on*-axis and a ray at x is given by

$$\Delta\varphi = \frac{2\pi}{\lambda_0} n_a t\{\tfrac{1}{2}a_2x^2 + \tfrac{1}{2}a_4x^4 \cdots\}. \tag{48}$$

We require t in (48) to be so small that

$$\Delta\varphi \ll \frac{\pi x}{\lambda} \tag{49}$$

and we represent the segment of focusing medium as a thin lens; for any thin lens the focal length f is

$$f = \frac{\pi x^2}{\lambda_0 \Delta\varphi}. \tag{50}$$

Then, combining (50) and (48),

$$f = \frac{1}{n_a l\{a_2 + a_4x^2 + a_6x^4 \cdots\}}. \tag{51}$$

If $a_2 = 0$, the focal length approaches infinity as $|\, x \,| \to 0$.

If the medium is represented mainly by the square law term a_2 with a small a_4 perturbation

$$f = \frac{1}{n_a t a_2(1 + R)} \tag{52}$$

where

$$R = \frac{a_4x^2}{a_2}. \tag{53}$$

The ratio (53) appears repeatedly in describing slightly non-ideal media.

VI. NORMAL MODE PROPERTIES IN ARBITRARY FOCUSING MEDIA

It would be nice to have solutions to Maxwell's equations for a medium according to (35) and (36) but this has not yet been achieved. E. A.

Marcatili has solved Maxwell's equations and found normal mode field properties for the ideal square-law medium (only a_2 present),[7] and for a perturbation thereon (small a_4 in a medium principally characterized by a_2).[8]

In this section, an approximate method for obtaining some of the properties of the modes of an arbitrary medium (pure fourth order, for example) is described. This is of interest as guidance on whether or not to put the effort into getting better solutions.

We use as limiting cases the solutions found by Marcatili when only a_2 is present, and the known solutions for a step transition in dielectric constant, which as previously noted in connection with (42) corresponds to a very high exponent on the x^n term of (36). These two cases can be viewed as limits to the possible solutions for arbitrary (36), within the bounds of (40), and useful results inferred about the intervening cases.

We note that the transverse field distribution for the first-order mode with the step-change of index, Curve I of Fig. 9, is of the form

$$E = \cos\left(\frac{\pi x}{2a}\right) \tag{54}$$

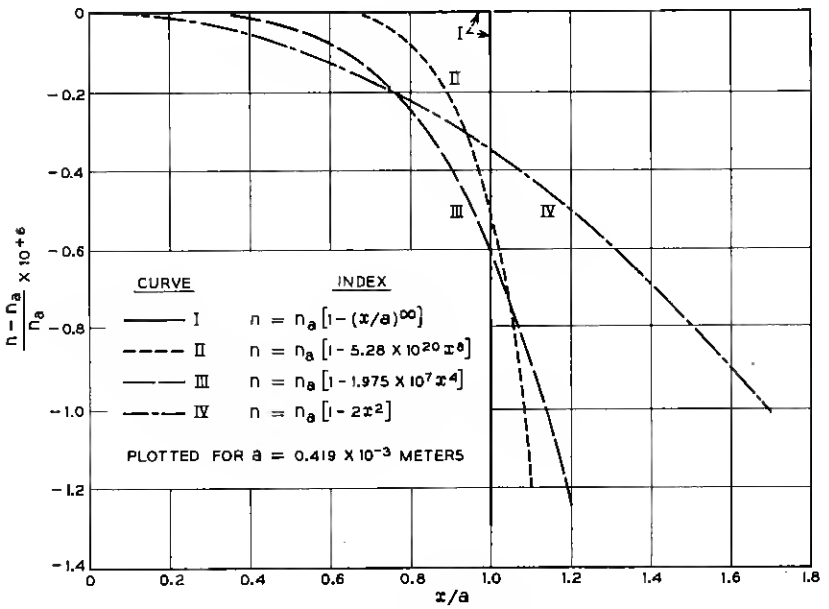

Fig. 9 — Index of refraction versus normalized transverse position (x/a) for several media.

where the index change occurs at $x = \pm a$. From Marcatili's wave solution,[7] the transverse field shape for the lowest order mode in a medium characterized by

$$n = n_a (1 - \tfrac{1}{2} a_2 x^2) \tag{55}$$

is given by

$$E = \exp\left[-\left(\frac{x}{\bar{x}}\right)^2\right] \tag{56}$$

where

$$\begin{aligned} \bar{x} &= \sqrt{\frac{\lambda}{\pi}} \frac{1}{(a_2)^{\frac{1}{4}}} \\ \lambda &= \lambda_0 / n_a \\ \lambda_0 &= \text{free space wavelength.} \end{aligned} \tag{57}$$

We now match the fields given by (54) and (56) by setting (54) equal to (56) at $x = \bar{x}$; this yields

$$a_e = 1.315\, \bar{x} \tag{58}$$

where a_e is an "equivalent" or effective half-width for the square-law medium. The corresponding field shapes and plots of index variation are given by Curves I and IV in Figs. 9 and 10.

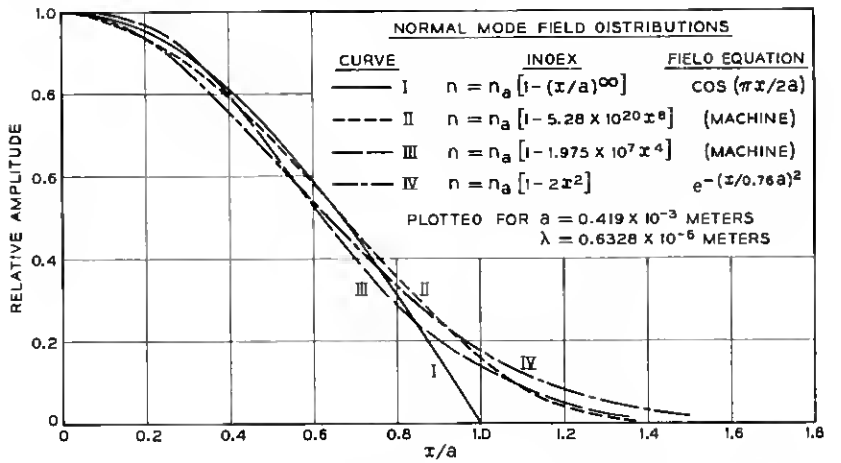

Fig. 10 — Normal mode amplitude vs normalized transverse dimension (x/a) for media of Fig. 9.

As already indicated, these two cases are limits on the index variation. It is inferred that an arbitrary index distribution (35) will have a field distribution similar to that of Curves I and IV of Fig. 10 when x is related to the effective width a_e to yield an index variation approximating Curves I and IV of Fig. 9. This idea has been carried through to specify a procedure for defining a_e for arbitrary media, and to yield particular solutions for several specific index variations. Approximate phase constants for the various modes of arbitrary media are also found.

To document the inference on normal mode field shape for the non-ideal medium, two specific cases were considered in a little more detail. These were represented by Curves II and III of Figs. 9 and 10. Pure fourth order and pure eighth-order index variations were taken, the constant a_n in (36) being selected to give an "eye-ball" fit to Curves I and IV of Fig. 9; the actual numbers for $(a_n/2)$ are on Fig. 9. Then, using the computer-simulation of a resonator as first employed by Fox and Li,[9] the normal mode field distributions were computed. More will be said about these calculations presently, but for now we note the conclusion on the normal mode field distributions for the eighth-order and fourth-order index variations, Curves II and III of Fig. 10. The choice of a_n for these curves was a first guess, not an optimized choice. Nevertheless, the fields do correspond very well to the limiting cases, Curves I and IV. We shall see that differences between Curves I, II, III, and IV in the region $x < 0.9a$ are comparable to the differences between the true fields in the system of ideal lenses and the Gaussian approximations commonly used to represent them.

The effective medium width a_e can be defined for a more general non-ideal medium as follows: the normal mode in the medium characterized by (35), (36) and (40) will have a shape similar to that of the associated square-law medium or step-change medium when a_e is defined by

$$f(x = a_e) = -r \frac{(1.315)^4}{2\pi^2} b^4 \left(\frac{\lambda}{a_e}\right)^2. \tag{59}$$

This comes from making $f(x)$ of (35) for the arbitrary medium equal to r times the same quantity for an equivalent square-law medium, both at $x = a_e$, and then using (57) and (58) to eliminate the a_2 of the equivalent square-law medium. The constant b is unity for the lowest order mode, and is shown in Appendix I to be

$$b = \sqrt{\frac{m + 2.5}{2.5}} \tag{60}$$

for the TEM_m mode.* The constant r varies slightly depending on the exact form of $f(x)$; in the examples plotted in Fig. 9, r is 1.72 for the fourth order case and 1.43 for the eighth order case. When considering a medium which is very nearly square law, r may be taken as unity, and for fourth or higher order media a value $r = 1.5$ is a good value.

Following known theory for metallic waveguides, the normal mode for the step-change index can be represented by two plane waves travelling at an angle α to the axis of the medium, where

$$\sin \alpha = \frac{\lambda}{\lambda_c} \tag{61}$$

and λ_c is the cutoff wavelength in the guide containing everywhere the index n_a. Restricting our interest to the region $\lambda/\lambda_c \ll 1$, the phase constant is given by

$$\beta = \frac{2\pi}{\lambda}\sqrt{1 - \sin^2 \alpha} \cong \frac{2\pi}{\lambda}\{1 - \tfrac{1}{2}\alpha^2\}. \tag{62}$$

Higher modes are accounted for by noting

$$\lambda_c = \frac{4a}{(m+1)} \tag{63}$$

giving

$$\begin{aligned} \beta &= \frac{2\pi}{\lambda}\left\{1 - \frac{1}{32}\left(\frac{\lambda}{a}\right)^2 (m+1)^2\right\} \\ \lambda &= \lambda_0/n_a . \end{aligned} \tag{64}$$

Since the principal part of the field distribution has been shown to be essentially the same for all $f(x)$ restricted by (40) provided a_e is defined as in (59), we can expect that the expression (64) will give a good approximation for the phase constant in a medium characterized by any $f(x)$.

We proceed to write down the expressions which result.

For the medium described by

$$n = n_a (1 - \tfrac{1}{2}a_2 x^2 - \tfrac{1}{2}a_4 x^4) \tag{65}$$

the application of (59) leads to

$$a_e = 1.315b\left[\frac{r}{a_2(1+R)}\right]^{\frac{1}{4}}\sqrt{\frac{\lambda}{\pi}} \tag{66}$$

* Following Fox and Li and Boyd and Gordon[10] the mth order mode has $(m+1)$ field maxima in the transverse cross section.

with $R = a_4 a_e^2/a_2$. The ratio R is the ratio of the fourth order term $0.5\ a_4x^4$ to the second order term $0.5\ a_2x^2$ at $x = a_e$, the equivalent half-width of the medium. Thus the expression (66) gives a_e implicitly.

When $R \ll 1$, we can rewrite $(1 + R)^{\frac{1}{2}} = 1 + \frac{1}{2} R$; under this condition, putting (66) into (64) gives for the medium characterized principally by a square-law distribution with small fourth-order variation, (taking $r = 1$),

$$\beta = \frac{2\pi}{\lambda} - 0.357 \sqrt{a_2} \left\{ \frac{(m+1)^2}{\left(\frac{m+2.5}{2.5}\right)} + \frac{0.275(m+1)^2 a_4 \lambda}{a_2^{3/2}} \right\}. \quad (67)$$

We can compare this result to Marcatili's direct wave solution[7] in the limit of $a_4 = 0$. The functional dependence on λ and a_2 is identical; the coefficient of $\sqrt{a_2}$ in (67) compares to the correct one as follows:

	Coefficient of $\sqrt{a_2}$	
m	Marcatili[7]	Eq. (67)
0	0.5	0.357
1	1.5	1.02
2	2.5	1.78
3	3.5	2.6
4	4.5	3.43
$m \to \infty$	m	$0.892\ m$

Thus, the approximate value of the phase constant is correctly given for all modes at any wavelength by the approximate theory outlined above, but the unique integral relationship for the phase differences between the modes in the square-law medium is not given.

A comparison between (67) and some unpublished results Marcatili obtained using a direct perturbation solution of Maxwell's equations shows identical dependence upon a_4, a_2 and λ with comparable but somewhat different constants.

The above comparisons lead one to have confidence in other results obtained from (59) and (64) for which there is no previous information. For example, we can get the phase constant corresponding to medium (65) with $a_2 = 0$. Equation (66) leads to

$$\begin{aligned} a_e &= \frac{r^{1/6}(1.315)^{2/3}}{\pi^{1/3}} \frac{b^{2/3} \lambda^{1/3}}{a_4^{1/6}} \\ &= 0.876 \left(\frac{m+2.5}{2.5}\right)^{1/3} \frac{\lambda^{1/3}}{a_4^{1/6}} \end{aligned} \quad (68)$$

for the equivalent half-width of the medium, and

$$\beta = \frac{2\pi}{\lambda} - 0.256(a_4\lambda)^{1/3} \frac{(m+1)^2}{\left(\frac{m+2.5}{2.5}\right)^{2/3}} \tag{69}$$

for the phase constant.

Likewise, for a medium

$$n = n_a(1 - \tfrac{1}{2}a_8x^8) \tag{70}$$

the application of (59) and (64) gives

$$\begin{aligned} a_e &= \left(\frac{r}{a_8}\right)^{0.1} \frac{(1.315)^{0.4}}{\pi^{0.2}} b^{0.4}\lambda^{0.2} \\ &= 0.925 \frac{\lambda^{0.2}}{a_8{}^{0.1}} \left(\frac{m+2.5}{2.5}\right)^{0.2} \end{aligned} \tag{71}$$

and

$$\beta = \frac{2\pi}{\lambda} - 0.323\lambda^{0.6}a_8{}^{0.2} \frac{(m+1)^2}{\left(\frac{m+2.5}{2.5}\right)^{0.4}}. \tag{72}$$

For the limiting case of a step change in index

$$\begin{aligned} a_e &= a \\ \beta &= \frac{2\pi}{\lambda} - \frac{\pi}{16}\frac{\lambda}{a^2}(m+1)^2. \end{aligned} \tag{73}$$

Looking at the change in β as the exponent in variation of index of refraction changes from 2 to 4 to 8 to ∞, (see (67) with $a_4 = 0$, (69), (72) and (73)), we observe that the β dependence on λ goes smoothly from λ^0 to $\lambda^{\frac{1}{4}}$, $\lambda^{0.6}$, and $\lambda^{1.0}$. It seems certain that the square-law medium is unique in having beats between modes being independent of λ.

There is a physical explanation for the increasing β dependence on λ for increasing exponent in the index variation. For the step change in refractive index the modes are all contained in the same transverse space, illustrated by Curves I of Figs. 11 and 12; by definition no energy can exist at $x > a$. However, with the square-law variation in refractive index, Curve IV of Fig. 9, energy can and does exist at $x > a_e$ and the penetration of the field at $x > a_e$ increases as the mode index m increases. This is illustrated for $m = 0$ and $m = 2$ as Curves II in Figs. 11 and 12 respectively. Since the higher order modes occupy more transverse width for increasing m, λ_c decreases more slowly for

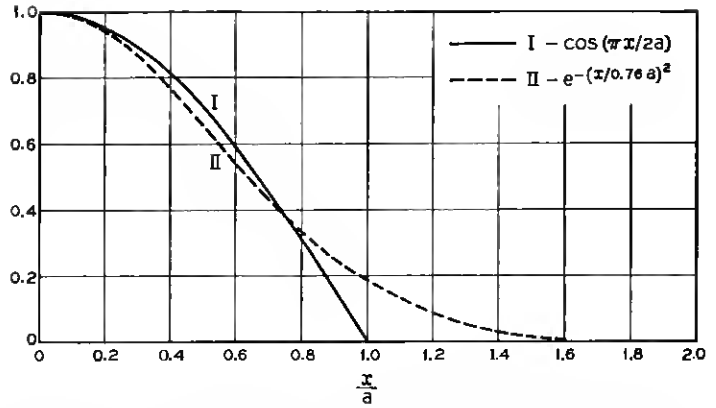

Fig. 11 — Normal mode amplitude versus normalized transverse dimension (x/a) for step change refractive index and square-law refractive index.

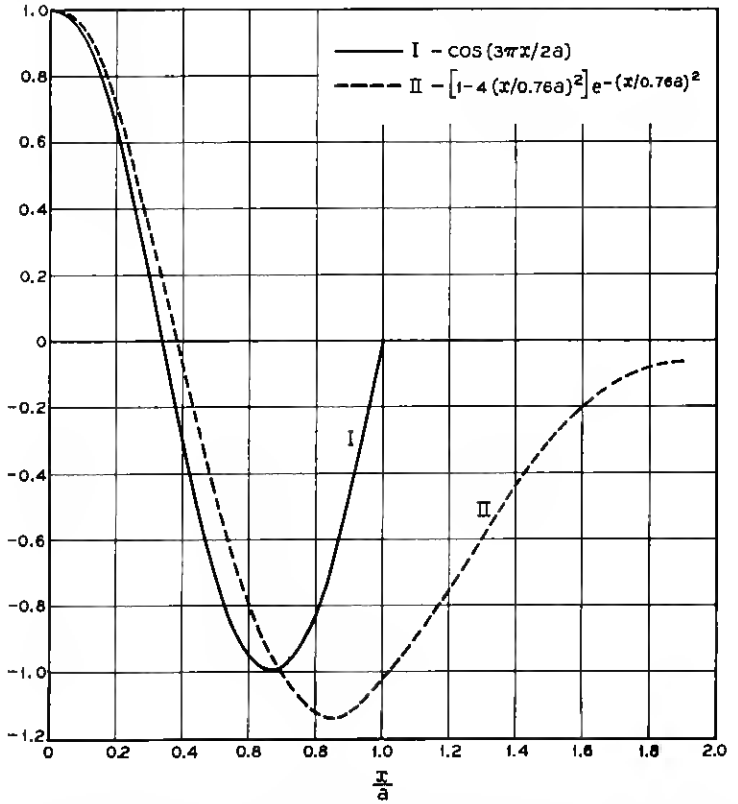

Fig. 12 — Normal mode amplitude versus normalized transverse dimension (x/a) for a higher-order mode in the step change index and square-law index media.

the square-law medium than for the step-change refractive index. That is the basic reason for the factor b, (60) appearing in (59). Similarly, the increased field penetration at $x > a_e$ for the square law compared to the step-change index makes the angle α smaller for the square-law medium than in the step-change medium, and consequently the β is less altered from the value $2\pi/\lambda$. As the exponent in the terms of $f(x)$ increases from 2 toward ∞ the behavior in β and λ_c approach those for the step-change medium because the more rapid variation in index at $x > a_e$ prevents the field from penetrating that region as much.

One can write explicitly an expression for tbe half-widtb w_e of the lowest order mode's field for the various non-square-law media using the relation

$$w_e = \frac{a_e}{1.315} \tag{74}$$

where a_e is again defined by (59). As a consequence of the method of defining a_e, (74) gives the exact spot size for the pure square-law medium. For the medium which is principally square law with a small fourth-order term, (65) with $R < 1$,

$$w_e = \sqrt{\frac{\lambda}{\pi}} \frac{1}{a_2^{1/4}} \left\{ 1 - 0.55 \frac{\lambda a_4}{a_2^{3/2}} \right\}. \tag{75}$$

For the pure fourth-order medium,

$$w_e = 0.666 \frac{\lambda^{1/3}}{a_4^{1/6}} \tag{76}$$

and for the pure eighth-order medium,

$$w_e = 0.703 \frac{\lambda^{0.2}}{a_8^{0.1}}. \tag{77}$$

It is possihle now to specify unique rays to consider characteristic of the particular mode in each of the media. These rays are the normals to the two plane waves which in combination give approximately the transverse field distributions in the manner outlined above. Each of these normals makes an angle α to the axis of the medium as in equation (61). Again confining our interest to waves far from "cut-off"

$$\alpha \cong \frac{\lambda(m+1)}{4a_e} \tag{78}$$

where a_e is again defined by (59). For the medium (65) with $R < 1$

$$a_e \cong \frac{1.315}{a_2^{1/4}} \sqrt{\frac{m + 2.5}{2.5}} \sqrt{\frac{\lambda}{\pi}} \left\{ 1 - 0.55 \left[\frac{m + 2.5}{2.5} \right] \frac{\lambda a_4}{a_2^{3/2}} \right\} \quad (79)$$

and

$$\alpha = \frac{\sqrt{\lambda}\, a_2^{1/4}}{2.97} \frac{(m + 1)}{\sqrt{\frac{m + 2.5}{2.5}} \left\{ 1 - 0.55 \frac{\lambda a_4}{a_2^{3/2}} \left(\frac{m + 2.5}{2.5} \right) \right\}}. \quad (80)$$

This expression also gives the characteristic ray angles for the square law medium by letting $a_4 = 0$.

For the fourth-order medium, (68) gives a_e and the characteristic ray angle is

$$\alpha = 0.285 \lambda^{2/3} a_4^{1/6} \frac{(m + 1)}{\left[\frac{m + 2.5}{2.5} \right]^{1/3}}. \quad (81)$$

For the eighth-order medium, (71) gives a_e and the characteristic ray angle is

$$\alpha = 0.271 \lambda^{0.8} a_8^{0.1} \frac{(m + 1)}{\left[\frac{m + 2.5}{2.5} \right]^{0.2}}. \quad (82)$$

Having a characteristic half-width a_e and ray angle α for each medium, we can easily calculate a characteristic ray period for each medium. With reference to Fig. 13, the ray at an angle α with the z axis has a period λ_p

$$\lambda_p = \frac{4a_e}{\alpha}. \quad (83)$$

For the pure square-law medium, using (66) and (80)

$$\lambda_p = \frac{4 \times 1.315 \times 2.97}{\sqrt{\pi}} \frac{1}{a_2^{\frac{1}{2}}} \left[\frac{m + 2.5}{2.5} \right] \frac{1}{(m + 1)} \quad (84)$$

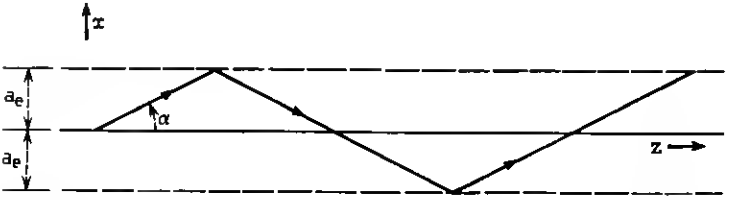

Fig. 13 — Diagram for determining an equivalent ray period in non-square-law media.

or

$$\lambda_p = \frac{8.8}{a_2^{\frac{1}{2}}} \frac{(m + 2.5)}{2.5(m + 1)}. \tag{84a}$$

We can compare this ray period to that derived from the paraxial ray equation; that solution is (10) from which the ray period is seen to be $2\pi/\sqrt{a_2}$. Equation (84a) corresponds quite well to $2\pi/\sqrt{a_2}$ for the lowest order mode ($m = 0$) including independence of λ! Equation (84a) is also relatively independent of mode order, m.

For the pure fourth-order medium the ray period from (83) is

$$\lambda_p = \frac{12.3}{\lambda^{1/3} a_4^{1/3}} \left[\frac{m + 2.5}{2.5}\right]^{2/3} \frac{1}{(m + 1)}. \tag{85}$$

There is no previous theory for comparison and, as already noted, ray theory alone does not define a unique period; unlike the square-law case, it depends on the initial ray slope.

VII. Field Distribution and Diffraction Losses in Resonators and Lens Waveguides Using Non-Square-Law Elements

In this section there are recorded new computations of normal mode field distributions and diffraction losses for a few resonators using non-spherical mirrors. The results are applicable to lens waveguides using non-square-law focusing elements. No other information is known to be available on these configurations.

The motivation for the work was to determine the normal-mode field distributions for non-square-law continuous waveguides to support the approximations made in the preceding section. Thus, most of the conditions selected represent relatively close spacing of weak lenses. A few instances are cited where cutoff effects associated with too great spacing of lenses were observed.

The resonator whose descriptive dimensions are given in Fig. 14 is to be used to represent the lens guidance system of Fig. 15. The equivalence is exact if one includes the absorbing screens in Fig. 15; if the diffraction losses in the resonator are not large very little effect is expected from omitting the absorbing screens. Fig. 15, in turn, can represent a continuous guidance medium when the focal length of the lenses is appreciably greater than the lens spacing. Then the beam size is very nearly the same at the lens and at the plane midway between lenses, and the electrically thin lenses of Fig. 15 can be representations of segments of the continuous medium of length s. For the square-law medium, this approximation is that the focal length expression (16) is

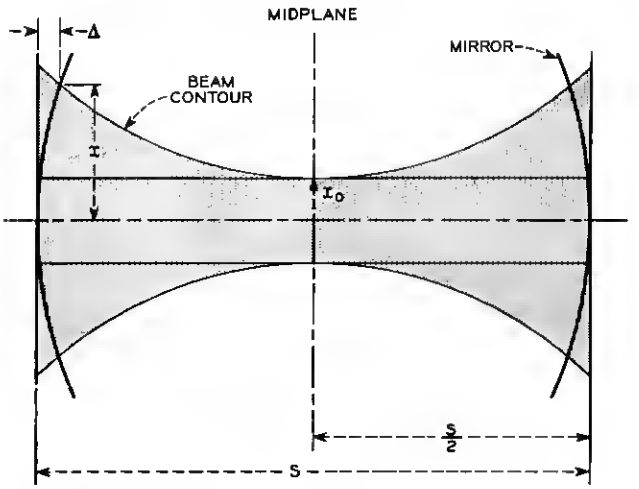

Fig. 14 — Definition of parameters in a resonator for use in Fox-Li type calculations.

well represented by

$$f = \frac{n_0}{n_a a_2 t} \tag{86}$$

when $\sqrt{a_2}\, t \ll 1$.

In representing a continuous medium by a resonator it is important to have a measure of the accuracy of the approximation. We obtain this and observe an interesting outcome by comparing the phase shifts along equi-power contours (i.e., contours within which the fraction of the total power in the beam is constant) for the resonator with spherical

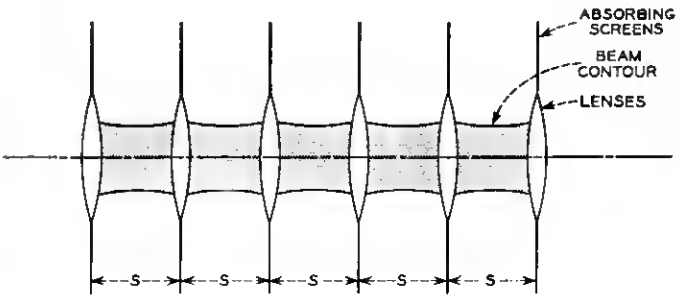

Fig. 15 — Transmission medium analogous to Fig. 14.

mirrors and for the square-law continuous medium,

$$n = n_a\ (1 - \tfrac{1}{2}a_2x^2). \tag{87}$$

For the square-law medium of length s, the phase difference for a ray following the axis and one at radius x_0 is

$$\Delta\varphi_c = \frac{2\pi}{\lambda_0}\, s(-\tfrac{1}{2}a_2{x_0}^2)\,. \tag{88}$$

For the resonator with spherical mirrors the phase difference between a ray on axis and one following an equi-power contour is

$$\Delta\varphi_m \cong \frac{2\pi}{\lambda_0}\,(-2\Delta)\,. \tag{89}$$

By making

$$\Delta = \frac{a_2 s}{4}\,x^2 \tag{90}$$

it is apparent that (88) and (89) are identical when $x = x_0$. It may be shown that the beam spot size at the center of the resonator is the same as the spot size of the continuous medium when

$$w_0 = \sqrt{\frac{\lambda}{\pi}\,\frac{1}{a_2^{\frac{1}{2}}}} = \sqrt{\frac{R_c\lambda}{2\pi}} \tag{91}$$

where R_c is the field curvature at the confocal spacing of mirrors associated with the mid-plane spot size w_0.* The equi-power contours are given by

$$\frac{x}{x_0} = \frac{w_s}{w_0} = \sqrt{1 + \xi^2} \tag{92}$$

$$\xi = \frac{s}{R_c} \tag{93}$$

w_s = spot size at the mirrors.

Using (91), (92), and (93), the value of *both* (88) and (89) is

$$\Delta\varphi_m = \Delta\varphi_c = \frac{4\pi}{\lambda_0}\,{x_0}^2\,\frac{s}{{R_c}^2}. \tag{94}$$

Thus by choosing the continuous medium and spherical mirror system to have the same mid-plane spot size, the phase shift along any contour enclosing equal powers is identical, regardless of lens spacing.†

* See Ref. 10.

† Within, of course, the region of stability for the resonator.

For reference it may be noted that the mirror radius of curvature b' and focal length f are related to R_c and s by[10]

$$b' = 2f = \frac{(1 + \xi^2)R_c}{2\xi} \tag{95}$$

$$R_c = \frac{2}{\sqrt{a_2}} = \sqrt{2sb' - s^2}. \tag{96}$$

Useful forms giving the mid-plane spot size w_0 and spot size at the lens w_s for the lens system of Fig. 15 are:

$$w_0 = \sqrt{\frac{\lambda}{2\pi}}\,(4fs - s^2)^{\frac{1}{4}} \tag{97}$$

$$w_0 = \sqrt{\frac{\lambda}{\pi}}\,(fs)^{\frac{1}{4}}\left(1 - \frac{s}{4f}\right)^{\frac{1}{4}} \tag{98}$$

$$w_s = \sqrt{\frac{\lambda}{\pi}}\,\frac{(fs)^{\frac{1}{4}}}{\left(1 - \frac{s}{4f}\right)^{\frac{1}{4}}}. \tag{99}$$

It seems certain from (94) that the normal mode field distribution for a continuous medium will be well represented by the normal mode of a resonator having the proper correspondence between Δ (Fig. 14) and the coefficients of (36), provided that the mid-plane of the resonator field does not differ appreciably from the field at the mirror.

The proper value for Δ of Fig. 14, to represent a general medium (35) and (36), is obtained by taking $x = x_0$ (Fig. 14) and letting $\Delta\varphi_m = \Delta\varphi_c$ as was done in connection with (88) and (89). This yields

$$\Delta = \frac{s}{2}\left(\frac{1}{2}\,a_2x^2 + \frac{1}{2}\,a_4x^4 + \frac{1}{2}\,a_6x^6 \cdots\right). \tag{100}$$

Selection of a mirror spacing suitably small can be done for the square-law medium with the aid of (92). For example, with

$$a_2 = 4 \text{ (meters)}^{-2}$$

$$s = 0.2 \text{ meters}$$

$$w_0 = 0.319 \times 10^{-3} \text{ meters}$$

$$R_c = 1 \text{ meter}$$

one computes $w_s/w_0 = \sqrt{1.04}$. This is based on the Gaussian function approximations for the actual fields. A computer determination of the

actual field distributions* has been carried out using the method of Fox and Li and the results are plotted in Fig. 16 for a Fresnel number $N = 1.38$.† These are true normal mode field distributions for the resonator; some perturbation from the Gaussian shape is caused by the 5.27 per cent power diffraction loss on each reflection but this does *not* account for the fact that the midplane $1/e$ width is approximately 7.5 per cent less than the mirror field instead of 2 per cent less as predicted by (92).

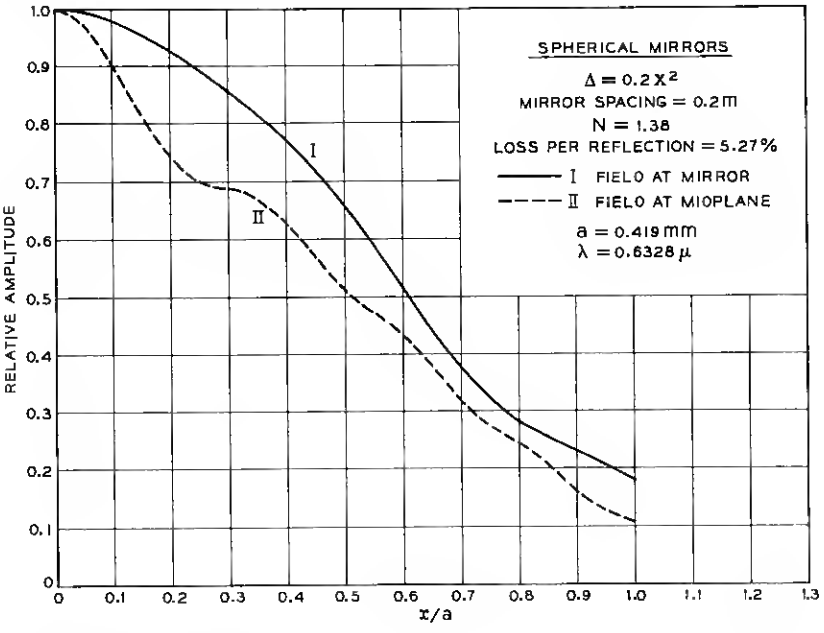

Fig. 16 — Computed normal mode fields at the mirrors and at midplane for a spherical mirror resonator.

See Fig. 17, where the diffraction loss is increased by reducing the mirror size; the mirror spot size changes very little. Also see Fig. 18, where the fields, both the real fields developed on the computer simulation and the Gaussian theoretical approximation thereto, are plotted. We see here, with $N = 1$ where diffraction losses are less than 0.1 per cent per reflection, that the Gaussian approximation is too narrow at the mirrors

* In all of the computer determinations of field distributions and losses, 100 radial intervals were employed in representing the transverse field distribution.

† In the terminology of this paper, $N = r^2/s\lambda$ where $2r$ is the mirror diameter and s is the mirror spacing.

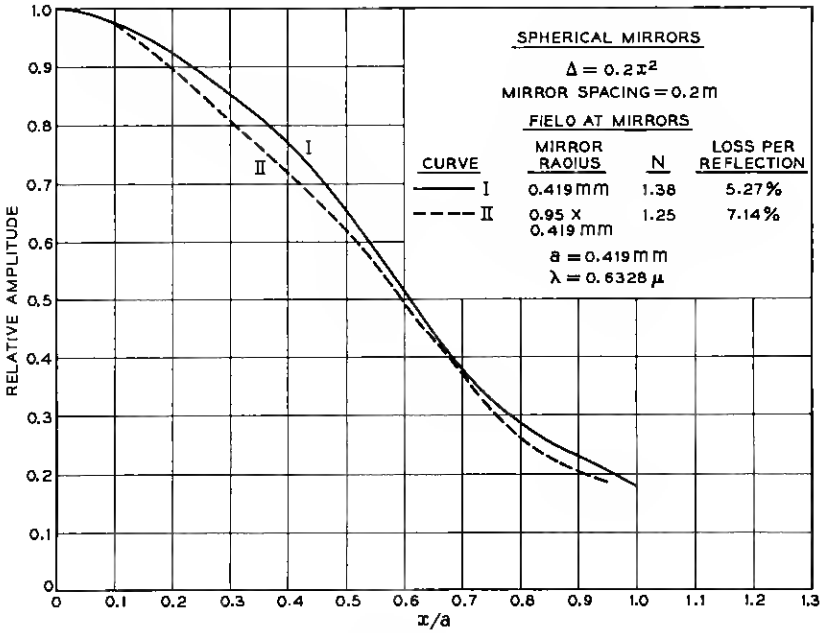

Fig. 17 — Computed normal mode fields at the mirrors for the resonator of Fig. 16 with two mirror diameters.

and too broad at the midplane; whereas $w_s/w_0 = \sqrt{2}$ from the Gaussian approximation, the actual ratio of widths at $1/e$ is about 1.58. The prolate spheroidal wave functions give computed results in much better agreement with the Fox-Li machine computation[10,11] and we presume the latter to be more accurate than the Gaussian approximation.

The transverse fields corresponding to the fourth-order index variation, Curve III of Fig. 9, is shown in Figs. 19 and 20. The mirror spacing, losses and Fresnel numbers are listed on the figures. The midplane field corresponds as well to the mirror field as did that for the square-law case, Fig. 16, and the spacing s is judged adequately short. For the same Fresnel number, $N = 1.38$ and the same spot size, the fourth-order medium had 3.91 per cent loss per reflection compared to 5.27 per cent for the square-law medium. This is because the field at $x = a_e$ falls off more sharply as shown on Fig. 10. The field plotted in Fig. 10 as Curve III was obtained from the computer data which produced Fig. 20, with the reflection number selected to minimize the amplitude of the higher modes still present in the data for Curve I of Fig. 20.

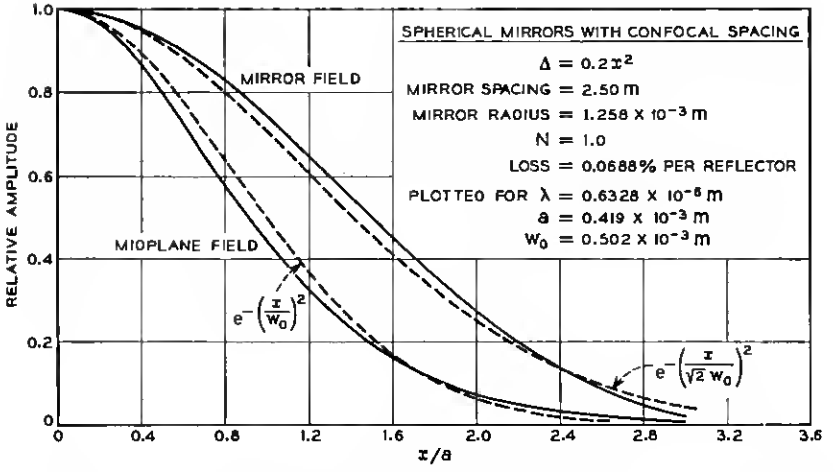

Fig. 18 — Comparison of normal mode fields in a confocal square law resonator as determined by (1.) Fox-Li type calculations and (2.) Gaussian analytical approximation.

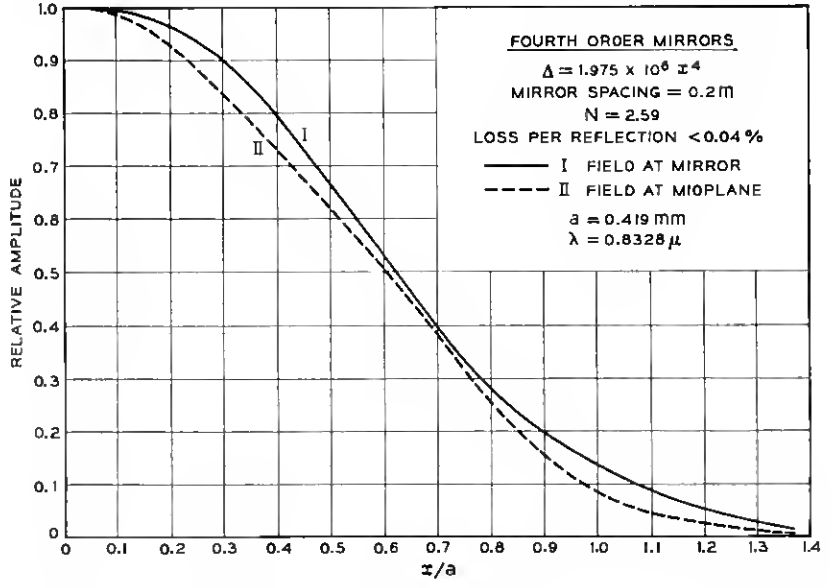

Fig. 19 — Computed normal mode fields at the mirrors and at midplane for a fourth-order mirror resonator.

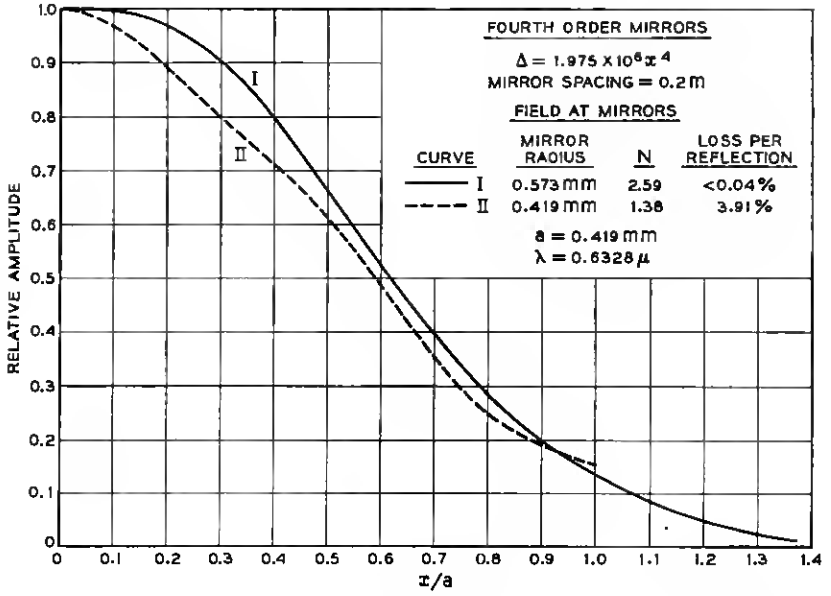

Fig. 20 — Computed normal mode fields at the mirrors for the resonator of Fig. 19 with two mirror diameters.

Figs. 21 and 22 show computed field distrihutions for a resonator with eighth-order mirrors chosen to match the medium of Curve II, Fig. 9, at the same mirror spacing used for Figs. 16–20, 0.2 meters. The value of Δ is computed from (100). In Fig. 21 we note the midplane field is quite unlike the mirror field, and in Fig. 22 we note the loss does *not* decrease smoothly for increasing mirror size, hut remains more or less independent of mirror size. This is due to the fact that the focal length, which is a function of radial position on the mirror according to (51), is too small compared to the mirror spacing at the outer edge of the mirror. For example, for the Curve III of Fig. 22, the focal length is 0.077 meters at the edge of the mirror. For larger mirrors than those represented in Fig. 22, it was found that hoth the loss and field distribution hecame constant, independent of mirror size. The fields striking the outer edges of these mirrors are radiated because they are reflected through the axis of the resonator at such a sharp angle as to miss the opposite reflector. Fig. 23 shows a rough sketch of this situation. (Note that the midplane fields resulting would he composed of a mixture of a propagating field and a radiated field.) An analogy can he made to the unstahle region which occurs for all rays in a resonator with spherical

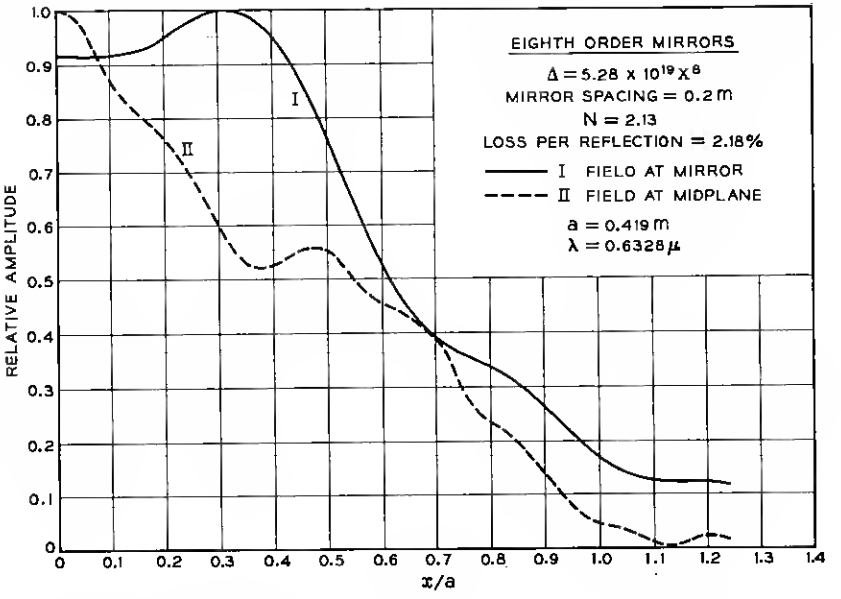

Fig. 21 — Computed normal mode fields at the mirrors and at midplane for an eighth-order mirror resonator.

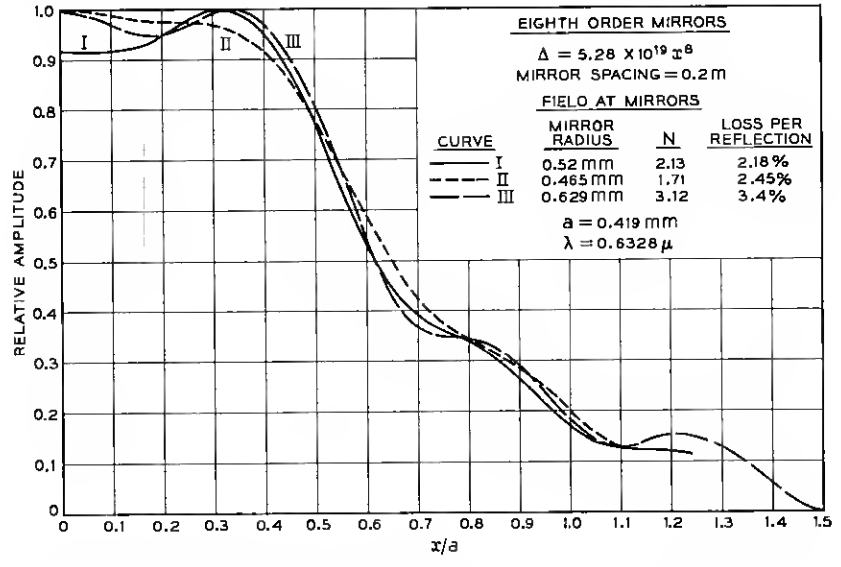

Fig. 22 — Computed normal mode fields at the mirrors for the resonator of Fig. 21 with three mirror diameters.

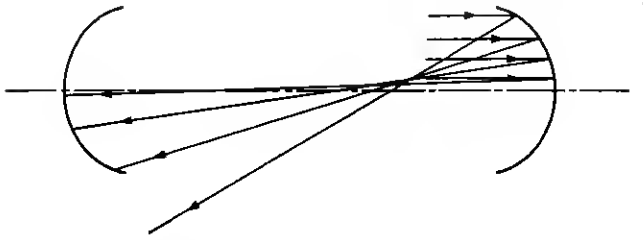

Fig. 23 — Diagram illustrating over-focusing losses in a resonator.

mirrors when $f < s/4$ or $f < 0.05$ meter when $s = 0.2$ meters as in Figs. 21 and 22.

The corresponding situation in a lens guidance system is shown in Fig. 24. The energy near the beam axis is weakly focused leaving a rather large spot size. The energy extending to larger and larger radii is eventually focused too strongly and misses the next focusing element, illustrated by the dotted lines of Fig. 24. Thus, ordinary field spreading, causing the usual diffraction losses, is mixed with over-focusing losses in a certain region of the parameters for a non-square-law resonator. It is believed that this accounts for the loss differences tabulated on Fig. 22.

The objective of determining the normal mode field for Curve II of Fig. 9 can be met by making the mirror spacing in the equivalent resonator smaller. This has been done in Figs. 25 and 26. In Fig. 25, the midplane field and mirror field are shown to agree quite well. In Fig. 26, some variation in field shape results with reduction in mirror size, but this is in part due to higher order modes still present in the field plotted for Curve I where the loss is extremely low. For the normal mode shape plotted as Curve II in Fig. 10, a careful selection of the resonator reflection number was made to minimize the higher-order mode amplitudes.

Using very closely spaced mirrors with so little curvature over the area where most of the beam energy is located, as in Curve II of Fig. 26

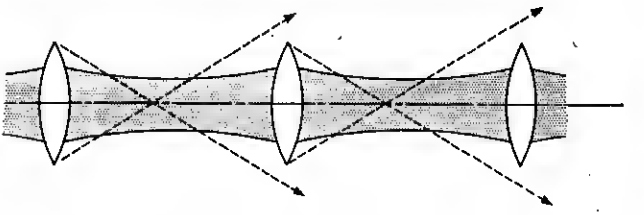

Fig. 24 — Diagram illustrating over-focusing losses in a lens guidance system.

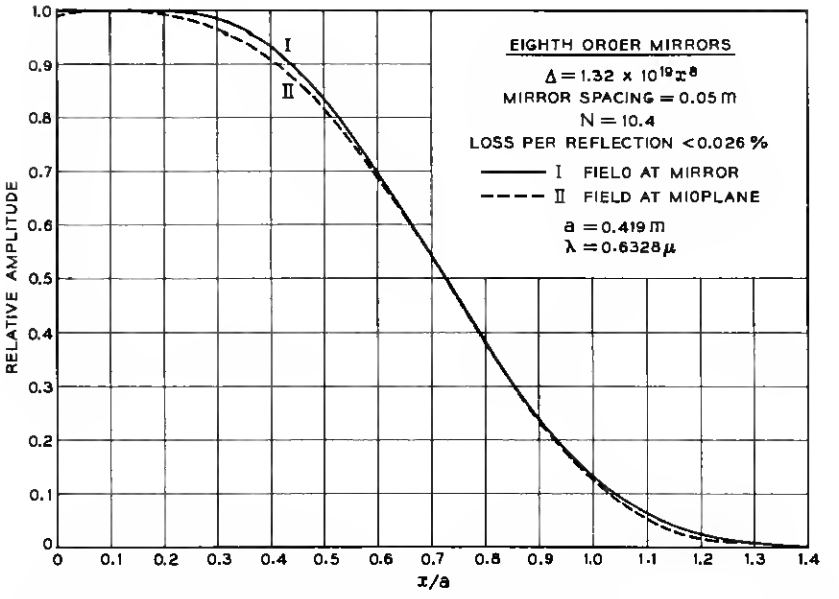

Fig. 25 — Computed normal mode fields at the mirrors and at midplane for an eighth-order mirror resonator representing a shorter segment of the same medium as in Fig. 21.

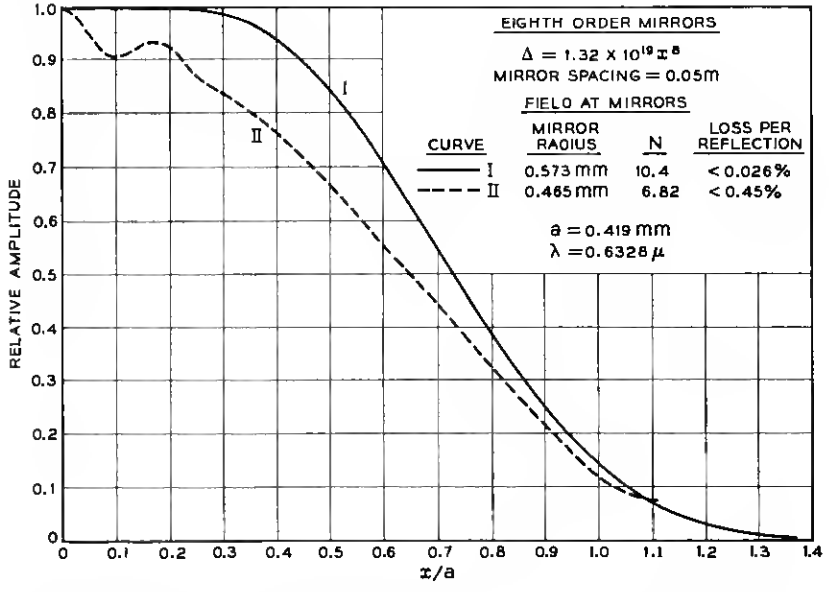

Fig. 26 — Computed normal mode fields at the mirrors for the resonator of Fig. 25 with two mirror diameters.

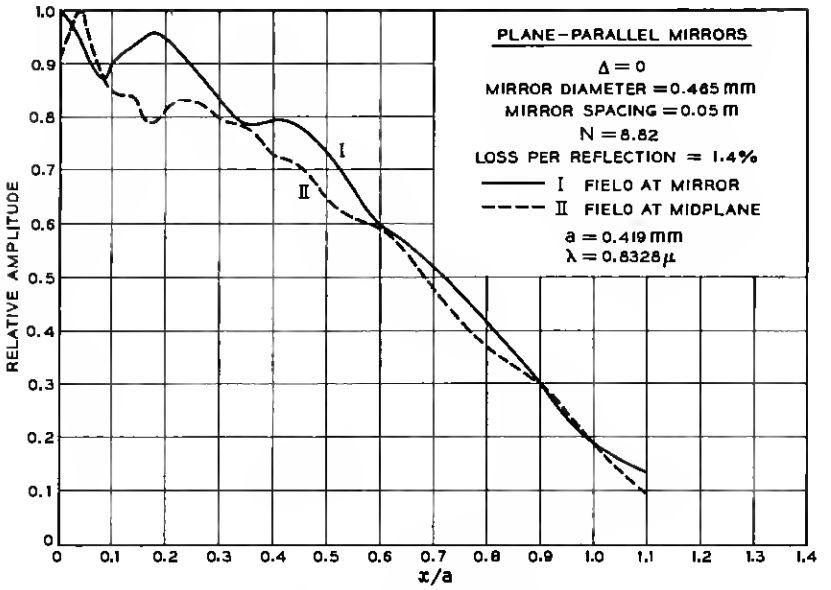

Fig. 27 — Computed normal mode fields at the mirrors and at midplane for a plane parallel mirror resonator analogous to the resonator of Fig. 25.

and the associate medium curvature curve II of Fig. 9, one might wonder whether the guidance is caused by diffraction as with plane parallel mirrors or really by the curvature of the mirrors. Fig. 27 shows the fields and loss for the plane-parallel mirrors corresponding exactly to Curve II of Fig. 26 for the eighth-order mirrors. The loss is <0.45 per cent for the eighth-order mirrors and 1.4 per cent for the plane parallel case. Evidently the guidance is importantly determined by the curvature.

VIII. RAY PATHS IN NON-SQUARE LAW MEDIA

In this section, the general properties of media described by (35), (36) and (40) are exploited to obtain approximate solutions for the paraxial ray equation (3) in several non-square-law media, and to indicate an approach which reduces to straightforward algebra the problems of getting similar solutions for other media.

It has been shown that (47) gives the general form of the ray path for the media of interest, and it was noted in connection with Fig. 7 that the limiting case of a step-shift in index of refraction results in a triangular waveform for the ray path. For a triangular waveform the coefficients b_m in (47) are in the ratio 1, 1/9, 1/25, etc. for $m = 1, 3, 5,$

etc. For the square law medium, a simple $\cos \beta z$ represents the ray path, as given in (7). Hence, we know that for any medium of interest the series (47) will converge very rapidly. We can hope to get a good approximation with only a few terms of (47). We now outline the results of such a solution for a medium described by (65). We set

$$x = c_1 \cos \beta z + c_2 \cos 3\beta z \tag{101}$$

which is equivalent to

$$\left.\begin{aligned} x &= x_0 \left\{ \left(1 + \frac{A}{4}\right) \cos \beta z - \frac{A}{4} \cos 3\beta z \right\} \\ x &= x_0 \{1 + A \sin^2 \beta z\} \cos \beta z \end{aligned}\right\} \tag{102}$$

with

$$A = - \frac{4 \frac{c_2}{c_1}}{\left(1 + \frac{c_2}{c_1}\right)} \tag{103}$$

$$\frac{c_2}{c_1} = - \frac{A}{4 + A} \tag{104}$$

$$c_1 + c_2 = x_0 . \tag{105}$$

In form (102) it is seen that the maximum x is x_0, occurring at $z = 0$, for any value of A; this is a useful form in visualizing the effect of a_4 as a perturbation on a medium mainly controlled hy a_2.

Using (101) we find

$$\frac{d^2}{dz^2}(x) = -c_1\beta^2 \cos \beta z - 9c_2\beta^2 \cos 3\beta z. \tag{106}$$

Also, from (65)

$$\frac{d}{dx}[f(x)] = -a_2 x - 2a_4 x^3. \tag{107}$$

We can get the solution to the paraxial ray equation in the form (43) by equating (106) to (107) with x replaced by (101). Equating the coefficients of the $\cos \beta z$ terms yields

$$\beta = \sqrt{a_2}\, \{1 + R(1.5 + 0.376A + 0.1875A^2)\}^{\frac{1}{2}} \tag{108}$$

where

$$R = \frac{a_4 x_0^2}{a_2} . \tag{109}$$

We note that the restriction (40) requires (107) to be greater than zero, or

$$R \geqq -\tfrac{1}{2}.$$

This is a limitation on x_0 if a_4 is negative.

Equating the coefficients of the cos $3\beta z$ terms gives

$$R = \frac{-0.89A}{\left[1.15A + 0.222\left(1 + \frac{A}{4}\right)^3\right]}. \tag{110}$$

Thus, with known R which is fully defined by the medium (a_2 and a_4) and the point of entry (x_0) for the ray, one can compute A and β. The plots of Figs. 28–30 show the interrelations between A, R, and β as given by (108) and (110). For $R \ll 1$, $A \cong -R/4$ and $\beta \cong \sqrt{a_2}\,(1 + 1.5R/2)$. The principal effect of a small a_4 term in the index variation is to change the period of the ray oscillation. This is illustrated in Fig. 31 for several values of R compared to the $R = 0$ (square law) case. Positive R means a_4 has a focusing effect, and the ray period is shortened.

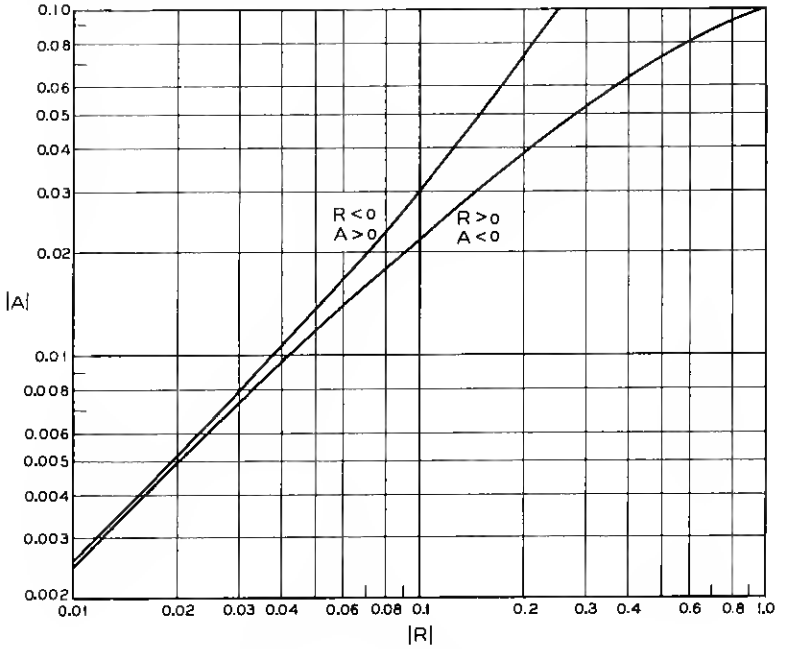

Fig. 28 — R vs A according to (110).

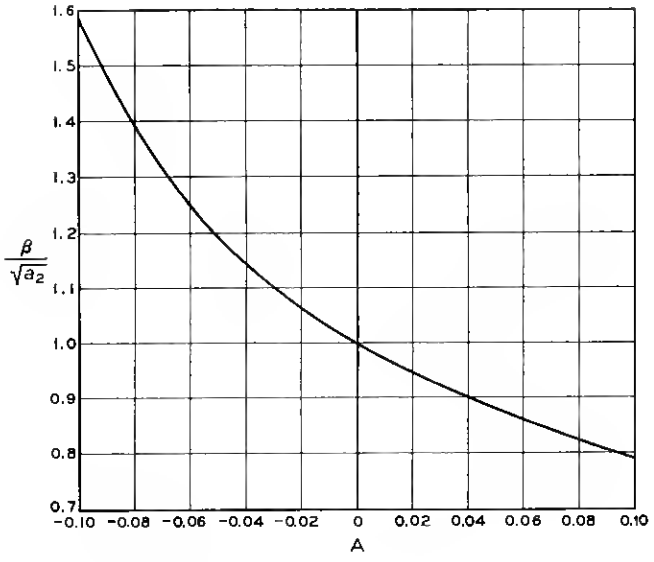

Fig. 29 — Normalized phase constant $\beta/\sqrt{a_2}$ vs A according to (108) and (110).

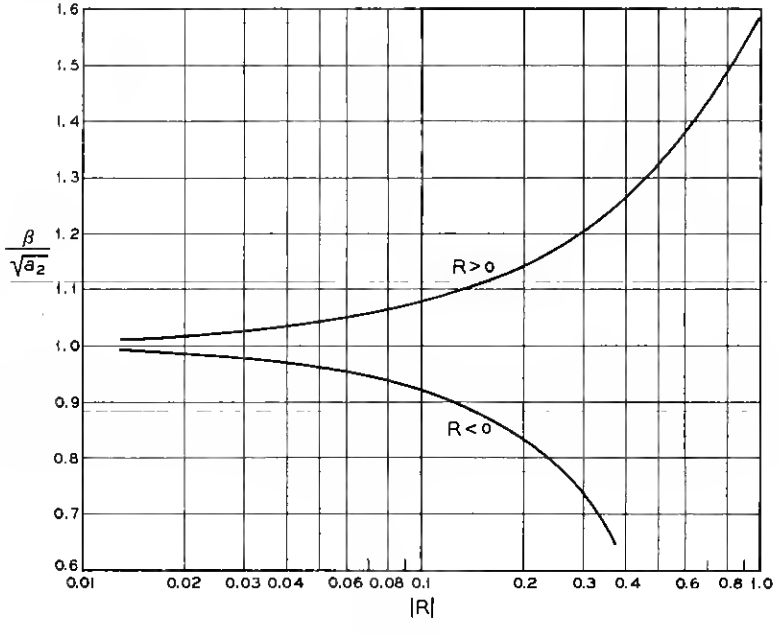

Fig. 30 — Normalized phase constant $\beta/\sqrt{a_2}$ vs R according to (108) and (110).

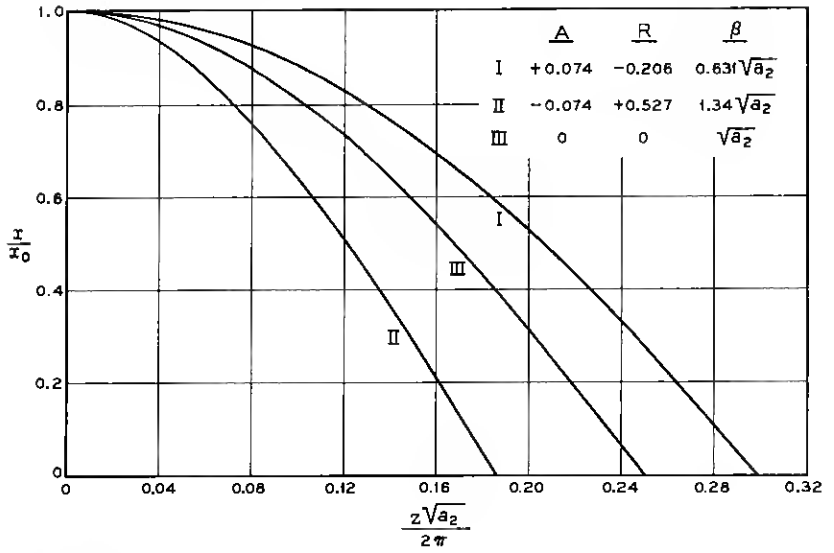

Fig. 31 — Ray position path x/x_0 vs normalized distance for a particular non-square-law medium.

With a renormalization of the abscissa, the curves of Fig. 31 are replotted in Fig. 32 to show that the cos $3\beta z$ term is indeed small and the ray path differs little from a sine wave.

However, the period $2\pi/\beta$ does depend on the peak ray-path amplitude (or ray-path slope at the axis), and hence the nice separation between the input-ray slope and input-ray position which was found in (10) does not exist for non-square law media.

Because the ray period depends on the peak ray-path amplitude, a group of rays entering a non-square law medium at $z = 0$ as in Fig. 33 will fall out of step and at some large z one ray will be at a positive maximum when another is at a negative maximum. These rays can represent parts of a beam of light injected into the medium off-axis when the beam spot size is very large compared to a wavelength. This shows that the injected off-axis beam will spread out and occupy the region $\pm w_t$ about the guide axis. However, the beam will never occupy any more than the region $\pm w_t$ if it is injected parallel to the guide axis.

One can obtain solutions analogous to the one given above if the input ray is on axis but at some slope x by noting

$$x = \Sigma c_n \sin n\beta z \tag{111}$$

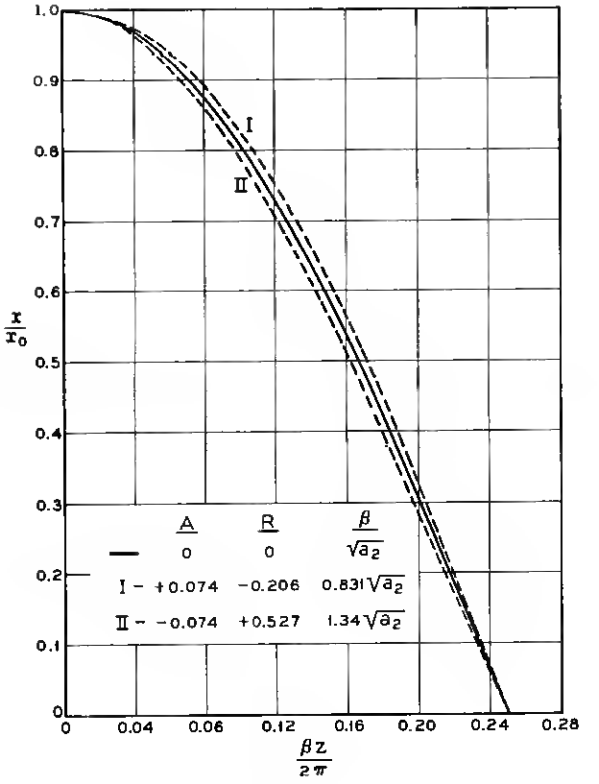

Fig. 32 — Ray position x/x_0 vs $\beta_2/2\pi$ for the medium of Fig. 31 showing basic similarity in shape of ray path.

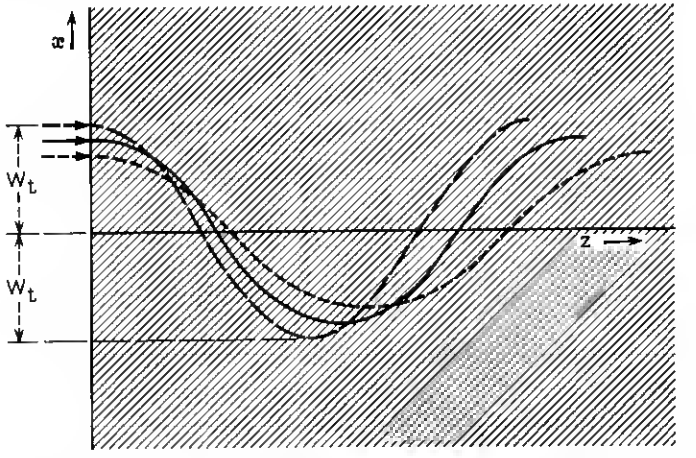

Fig. 33 — Ray position x vs distance z in a non-square-law medium illustrating the way an input beam breaks up as the wave propagates.

$n = 1, 3, 5$, etc. This follows from the same considerations which led to (47). Since we already have solved for the coefficients c_1 and c_2 of (101), we can get the solution for (111) by transforming (101), letting $x_1(z') = x(z - \pi/2\beta)$ which yields

$$x_1 = c_1 \sin \beta z - c_2 \sin 3\beta z. \tag{112}$$

The parameters c_1 and c_2 are related to x_0, the maximum of x_1, as in (105) and we define a new parameter B

$$B = \frac{12\left(\frac{c_2}{c_1}\right)}{1 - 3\left(\frac{c_2}{c_1}\right)} \tag{113}$$

which allows the ray slope to be written

$$\begin{aligned} \frac{dx_1}{dz} &= c_1\beta \cos \beta z - 3c_2\beta \cos 3\beta z \\ &= x_1' \left\{\left(1 + \frac{B}{4}\right) \cos \beta z - \frac{B}{4} \cos 3\beta z\right\} \\ &= x_1'\{1 + B \sin^2 \beta z\} \cos \beta z. \end{aligned} \tag{114}$$

The initial slope x_1' is the ray slope at $z = 0$, and it is related to c_1 and c_2 by

$$x_1' = c_1\beta \left\{1 - \frac{3c_2}{c_1}\right\}. \tag{115}$$

The previous interrelations between c_1, c_2, A, β, and R still hold. We seek a method for getting β and x_0, knowing only x_1, a_2 and a_4. To do so x_1', is rewritten in the form

$$x_1' = \frac{a_2}{\sqrt{a_4}} \sqrt{R}\,(1 + A)\{1 + R(1.5 + 0.376A + 0.1875A^2)\}^{\frac{1}{4}}. \tag{116}$$

Hence, given x_1', (116) determines $x_1' \sqrt{a_4}/a_2$ in terms of R (since R vs A is given in (110)); knowing R, a_2 and a_4, we can compute x_0 and β using (109) and (108). Fig. 34 sbows $x_1' \sqrt{a_4}/a_2$ vs R to facilitate this process.

For an input ray with both slope and displacement, tbe proper matcb-ing to (101) with a suitable transformation can in principle be done, but has not been attempted.

An approximate solution for the pure fourth-order medium

$$n = n_a(1 - \tfrac{1}{2}a_4x^4) \tag{117}$$

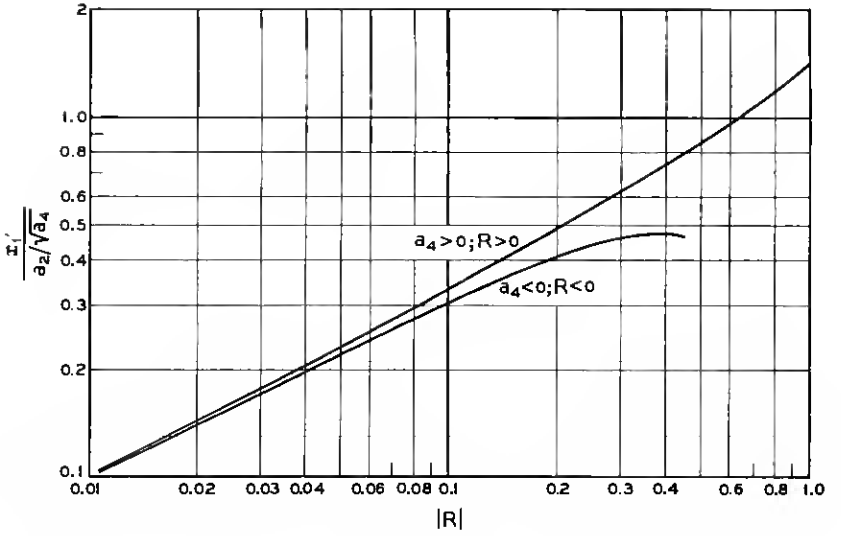

Fig. 34 — Normalized input ray slope x_1' vs R according to (116) and (110).

is obtained by letting $a_2 \to 0$ in the equations which led to (108) and (110). This yields

$$\beta = x_0 \sqrt{1.44 a_4} \tag{118}$$

$$\frac{c_1}{c_2} = 23.3 \tag{119}$$

$$A = -0.165 \tag{120}$$

for the solution corresponding to (101) and

$$x_1' = x_0^2 \sqrt{a_4} \tag{121}$$

for the solution corresponding to (114). Equation (121) gives the ray slope at the axis $x = 0$.

Better approximations would of course be obtained by including higher order terms in (101) but the large c_1/c_2 ratio produced by including only the cos $3\beta z$ terms suggests that the cos $5\beta z$ term would have a negligible coefficient.

We can combine (121) and (118) to express the ray period for the fourth-order medium in terms of the ray slope at the x-axis; this gives

$$\beta = a_4^{\frac{1}{4}} \sqrt{1.44 x_1'}\,. \tag{122}$$

We can now compare the ray period from (122) with that previously derived, (85). We let x_1' equal the characteristic ray angle defined by (81) with $m = 0$. Then the ray period from (122) becomes

$$\frac{2\pi}{\beta} = \frac{9.81}{\lambda^{\frac{1}{3}} a_4^{\frac{1}{3}}}. \tag{123}$$

The constant in (123) differs slightly from the value 12.3 found in (85) but the dependence on λ and a_4 is identical.

IX. DISCUSSION AND ACKNOWLEDGEMENT

The abstract contains a summing up review of the contents of this paper. One might add that a remarkably small step change in index is required to contain completely (for practical purposes) a light beam. As shown in Fig. 9, at $\lambda = 0.6328\ \mu$, a step change in index of refraction of a few parts in 10^6 is adequate for a beam radius of $a = 0.419$ mm, and this change need only be maintained from $x = a$ to $x \cong 2a$ where the energy is certain to be too small for that region to influence the wave propagation.

The author would like to thank Mr. Tingye Li for the use of his computer program which was modified to make the computations represented in Figs. 16–27. Without Mr. Li's previous work the author would not have included those figures which help justify the inferences leading to (59). Mrs. C. L. Beattie made the modifications and very effectively saw through all of the computations, for which the author is most appreciative. Mr. E. A. Marcatili on numerous occasions gave learned reactions to the newly developed ideas.

APPENDIX

We seek here to account for the expression (60)

$$b = \sqrt{\frac{m + 2.5}{2.5}}. \tag{124}$$

As noted in connection with Figs. 11 and 12, in a medium with a continuous variation in index of refraction, the fields of the higher order modes extend farther from the axis than do the fields of the lowest order mode. The technique used here to determine the phase constant and characteristic ray angle for rather general media is to establish an equivalent width of medium in which the energy is completely confined —as in guides with perfectly conducting walls or with zero permittivity

walls. It is clear then that this equivalent width must be different for the lowest-order modes than for higher-order modes.

When the author was casting about for a method of expressing this change, E. A. Marcatili pointed out that there is a characteristic radial distance at which the function describing the square-law medium's modes changes from an oscillating function to an exponentially decaying function. These functions are the parabolic cylinder functions and the value of x for the transition is*

$$x_t = 2\sqrt{m + \frac{1}{2}} \tag{125}$$

where m is the mode index.

This was tried as an equivalent width, but was found to change much more rapidly at small m than the actual increase in extent of the field illustrated in Figs. 11 and 12. By examining the radii at which the field decreased to about 1 per cent of the peak value for various low-order modes, it was found that (124) represents the variation quite well. Thus, the general form (125), which is supported by the function theory for the square-law medium, was modified to fit actual known field width variations at small m. For large m, (124) and (125) do have the same variation.

The method of defining the equivalent width, outlined in the body of the paper in connection with (59), causes media with higher than square-law variations in index to merge smoothly into the known behavior of the step-change index variation including the gradual disappearance of the factor b.

REFERENCES

1. Marcuse, D., Theory of a Tubular Gradient Gas Lens, Trans. MTT, Nov., 1965.
2. Marcuse, D., Private communication.
3. Pierce, J. R., Modes in Sequences of Lenses, Proc. Natl. Acad. Sci., *47*, 1961, pp. 1808–1813.
4. Pierce, J. R., *Theory and Design of Electron Beams*, second edition, D. Van Nostrand Co., 1954.
5. Miller, S. E., Alternating Gradient Focusing and Related Properties of Convergent Lens Focusing, B.S.T.J., *43*, July, 1964, pp. 1741–1758.
6. Marcuse, D., and Miller, S. E., Analysis of Tubular Gas Lens, B.S.T.J., *43*, July, 1964, pp. 1759–1782.
7. Marcatili, E. A. J., Modes in a Sequence of Thick Astigmatic Lens-Like Focusers, B.S.T.J., *43*, Nov. 1964, pp. 2887–2904.

* See *Handbook of Mathematical Functions with Formulas, Graphs, and Mathematical Tables*, U. S. Dept. of Commerce, National Bureau of Standards, Applied Mathematics Series, *55*, June, 1964, p. 690.

8. Marcatili, E. A. J., to be written.
9. Fox, A. G., and Li, T., Resonant Modes in a Maser Interferometer, B.S.T.J., *40*, March, 1961, pp. 453–488.
10. Boyd, G. D., and Gordon, J. P., Confocal Multimode Resonator for Millimeter Through Optical Wavelength Masers, B.S.T.J., *40*, March, 1961, pp. 489–508.
11. Slepian, D., Prolate Spheroidal Wave Functions, Fourier Analysis and Uncertainty-IV: Extensions to Many Dimensions; Generalized Prolate Spheroidal Functions, B.S.T.J., *43*, Nov., 1964, p. 3009.